European Journal of Protistology 102 (2026) 126181

Contents lists available at ScienceDirect

European Journal of Protistology

journal homepage: www.elsevier.com/locate/ejop

Scottish nearshore monothalamid Foraminifera (Rhizaria): Description of five new species and one new genus

Zaineb Henderson [a,*,1], Maria Holzmann [b,2], Andrew J. Gooday [c,d,3]

[a] School of Biomedical Sciences, Faculty of Biological Sciences, University of Leeds, Leeds LT2 9JT, UK
[b] University of Geneva, Department of Genetics and Evolution, Quai Ernest Ansermet 30, CH-1211 Geneva 4, Switzerland
[c] National Oceanography Centre, European Way, Southampton SO14 3ZH, UK
[d] Life Sciences Department, Natural History Museum, Cromwell Road, London SW7 5BD, UK

ARTICLE INFO

Keywords:
Morphology
Magnetic particles
DNA barcoding
SSU rDNA sequences
Northwest Scotland
Intertidal zone

ABSTRACT

Henderson (2023) gave informal descriptions of several soft-walled, monothalamid foraminifera from intertidal zones in the Lorne area of northwest Scotland based on morphology. In the present study, we use a combination of morphological and molecular data to formally establish one new genus and five new monothalamid species from the same area. *Lorneia sphaerica* gen. & sp. nov. (monothalamid Clade D) has a spherical, coarsely agglutinated test containing magnetic particles and minute aperture-like openings distributed around the test. *Lorneia ovalis* gen. & sp. nov. (Clade D) has similar characteristics, but the test is oval, and there is a terminal aperture situated at each end. *Psammophaga owensi* sp. nov. (Clade E) has an oval, finely agglutinated test with a simple terminal aperture and intracellular magnetic particles. In *Hilla brevis* sp. nov. (Clade Y), the test is broadly oval and finely agglutinated with a reflective sheen and a large terminal aperture with a pronounced collar. *Flaviatella zaninettiae* sp. nov. (Clade Y) has an elongate, finely agglutinated test with a reflective sheen, a tubular terminal apertural structure, and distinctive yellow cytoplasm. Two species, *Flexammina islandica* Voltski and Pawlowski, 2015 and *Ovammina opaca* Dahlgren, 1962, are reported for the first time in Scottish coastal waters. This study underlines the importance and diversity of monothalamid foraminifera in coastal settings.

1. Introduction

Foraminifera are single-celled eukaryotic protists classified as Rhizaria, which together with the Telonemia, Stramenopila, and Alveolata, belong in the TSAR supergroup (Burki et al., 2020). With the exception of a few 'naked' species, the cell body is enclosed within a test that is either single-chambered (monothalamous) or multichambered (polythalamous) (Loeblich and Tappan, 1987). Most research has concentrated on multichambered foraminifers, which have a superb fossil record, while the monothalamids, particularly the 'soft-shelled' species that have little fossilisation potential, have generally received much less attention. However, during the last few decades, there has been an upsurge of interest in monothalamids in all marine environments from estuaries to deep-sea trenches (Gooday, 2002; Gooday and Fernando, 1992; Gooday et al., 2008; Habura et al., 2008; Pawlowski and Holzmann, 2008; Sergeeva and Anikeeva, 2024). A few lineages have also been found living in terrestrial and freshwater environments (Holzmann et al., 2021; Lejzerowicz et al., 2010; Siemensma and Holzmann, 2023). An increasing number of new soft-shelled taxa have been described, in many cases using a combination of molecular and morphological data. These molecular phylogenetic studies have indicated that monothalamids form a paraphyletic group at the base of the foraminiferal evolutionary tree (Pawlowski et al., 2003, 2013).

Molecular and morphological studies have shown that the deep sea, and particularly the generally stable environments of the abyssal plains, host a vast diversity of largely undescribed single-chambered foraminifera (Barrenechea Angeles et al., 2024; Cordier et al., 2022; Glock, 2023; Goineau and Gooday, 2019; Gooday et al., 2020; Himmighofen et al., 2023; Pawlowski et al., 2011; Scheckenbach et al., 2009; Stachowska-Kaminska et al., 2022). Less attention has been paid to

* Corresponding author.
E-mail addresses: z.henderson@leeds.ac.uk (Z. Henderson), maria.holzmann@unige.ch (M. Holzmann), ang@noc.ac.uk (A.J. Gooday).
[1] https://orcid.org/0000-0001-8502-5861.
[2] https://orcid.org/0000-0003-2460-6210.
[3] https://orcid.org/0000-0002-5661-7371.

https://doi.org/10.1016/j.ejop.2026.126181
Received 4 November 2025; Received in revised form 5 January 2026; Accepted 5 January 2026
Available online 6 January 2026

monothalamids in estuarine and near-shore environments (Altin-Ballero et al., 2013; Ellison, 1984; Gooday et al., 2011; Gschwend et al., 2016; Habura et al., 2004, 2008; Pawlowski et al., 2008; Sergeeva and Anikeeva, 2024; Voltski and Pawlowski, 2015), with only a few reports originating from UK coastal waters (Larkin and Gooday, 2004; Siddall, 1880; Wilding, 2002). Nevertheless, a rich diversity of monothalamid species in estuarine areas on the French Atlantic coast was revealed recently by environmental DNA analyses (Singer et al., 2023). These more accessible habitats, which are some of the most dynamic systems in the marine realm, are particularly vulnerable to anthropogenic pollution and environmental changes (Day et al., 2012; Jorissen et al., 2022; Whitfield and Elliott, 2011), justifying further investigation of their monothalamid assemblages.

The west coast of Scotland is characterised by a diversity of fjordic loch, estuarine, open-ocean and island marine environments hosting ecosystems that are still relatively pristine and free of pollution, albeit increasingly subject to the pressures of tourism, marinas and fish farming. The Lynn of Lorne (or Lorn) area on the West coast of Scotland, opposite the Isle of Mull, has the advantage of not being too remote and is close to the research facilities at the Scottish Association for Marine Science (SAMS) in Oban. It therefore provides a good setting in which to enhance our knowledge of monothalamids living in Scottish near-shore habitats. Recently, an exploratory morphology-based study of estuarine and near-shore environments, located mainly around the mouths of sea lochs in the Lynn of Lorne, revealed a remarkable diversity of morphotypes (Henderson, 2023). Molecular characterisation of monothalamids in this general area had been carried out previously on samples from Dunstaffnage Bay (30–50 m depth), although without corresponding morphological data (Pawlowski and Holzmann, 2008; Pawlowski et al., 2008).

The aim of the current study is to use a combination of molecular and morphological characters to describe new taxa, including some of the species recognised in this earlier study (Henderson, 2023). Five new species and one new genus are described together with new records for two previously recognised species. Two of the new species, *Lorneia ovalis* and *Hilla brevis*, were not encountered by Henderson (2023). A third, *Flaviatella zaninettiae*, which was represented by a single specimen in this previous study, was subsequently found in abundance and described here in greater detail. *Flaviatella zaninettiae* shows a wide geographical and bathymetric distribution, as members of this species have also been sequenced from shallow water regions of Nuuk Fjord, Greenland, and deep-water regions of Vestnesa Ridge, Greenland Sea.

2. Materials and methods

2.1. Locations

The sampled areas on the northwest coast of Scotland, bordering the northeast Atlantic Ocean, have been described previously (Henderson, 2023). Those chosen for the current study include a bay next to the Lynn of Lorne, which extends along the east side of Loch Linnhe, and three bays around the mouths of the inner sea lochs Loch Etive and Loch Creran (Fig. 1). All are of an estuarine character; each being fed by a small river and with muddy sediment rich in worm casts. Site 1 in Loch Laich lies on the eastern side of Loch Linnhe (Fig. 1) and is the estuary of a river that runs through Glen Stockdale (Fig. 2A), partly over a bedrock of Dalradian limestone. Site 2 is located to the south of Site 1, on an extensive muddy tidal flat (Fig. 2B) facing the mouth of Loch Creran on its eastern flank and bordered by the Isle of Eriska on its northern side (Fig. 1). Site 3 is a small muddy bay further into and on the south side of Loch Creran (Fig. 1). The bedrock of Sites 2 and 3 is Dalradian schist. Site 4 is situated further south along the main coast, and on the southern side of the mouth of Loch Etive, located in Dunstaffnage Bay (Figs. 1, 2C). Here, the bedrock is composed of Silurian and Devonian igneous rocks. In all of these sites, free monothalamids were collected from patches of firm or sticky sediment close to the river and to the low tide line. A

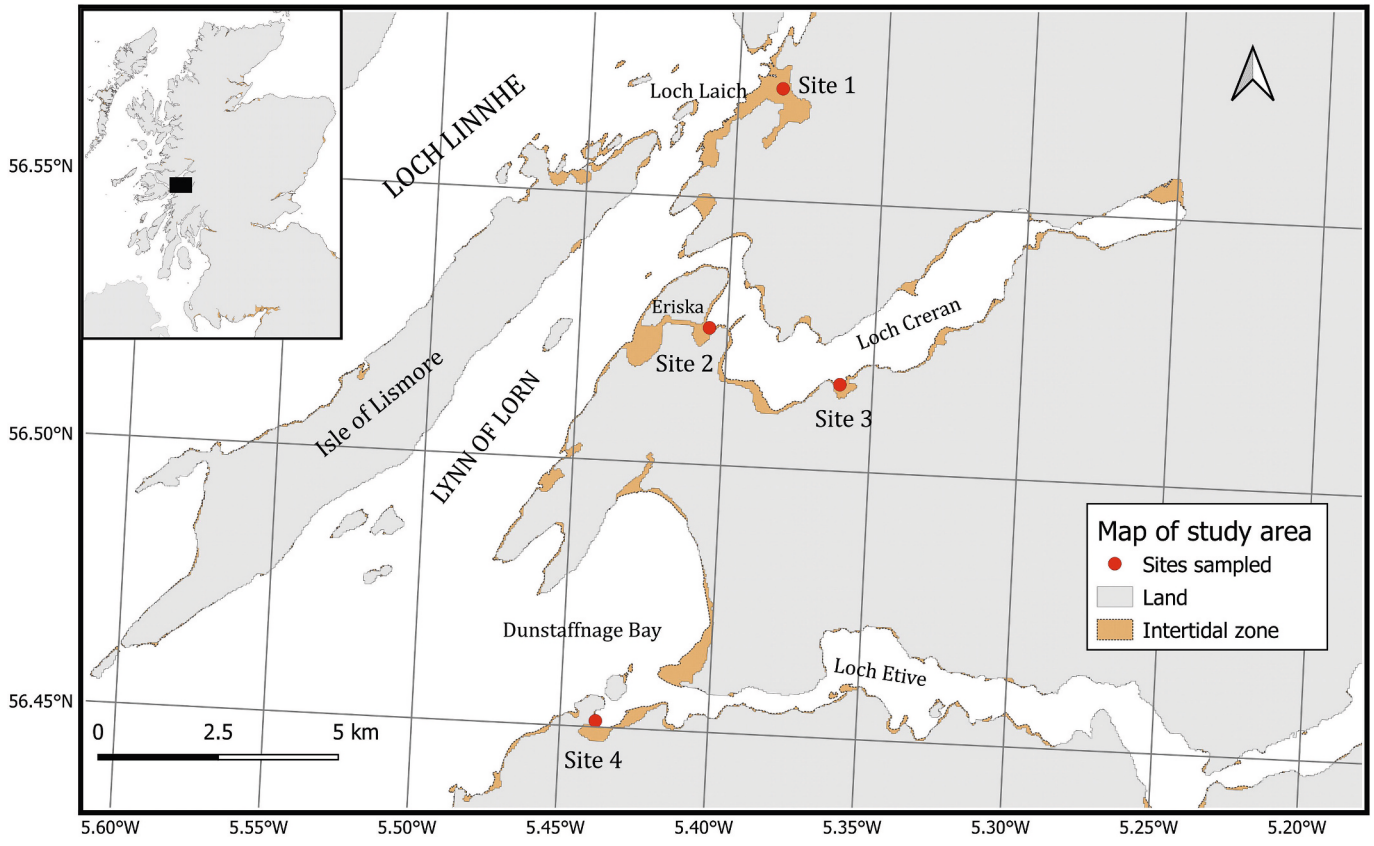

Fig. 1. Map of sampling sites in the Lorn area of north west Scotland.

Fig. 2. Appearance of three of the intertidal sampling sites. (**A**) Site 1 at Loch Laich. (**B**) Site 2 at Loch Creran, next to the Isle of Eriska. (**C**) Site 4 at Dunstaffnage Bay.

sessile species of monothalamid, *Flexammina islandica*, was attached to pebbles, seaweed, or empty bivalve shells near the tide line. Sample areas and sampling procedures for Nuuk Fjord, Greenland, and Vestnesa Ridge, Greenland Sea, have been described in detail by Gooday et al. (2022) and Holzmann et al. (2025b).

2.2. Sampling and processing of the specimens

Samples were collected as described previously (Henderson, 2023) between August 2023 and August 2024 from sediment, mudballs, seaweed, pebbles, or shells exposed at low tide (0.2–1.0 m height above chart datum; Table 1). Individual monothalamids were photographed and checked for the characteristic pseudopodia of foraminifera, as observation of the granulo-reticulopodia indicates live specimens. Low-power photomicrographs were taken of living monothalamids under a trinocular Nikon SMZ-10 dissection scope equipped with a Nikon D7000 SLR camera, and with a trinocular Leica M165c stereomicroscope equipped with a 5MEG L3CMOS05100PA Digicam. Micrographs and videos of pseudopods of living monothalamids and of intracellular details of specimens embedded in glycerol were taken with a Nikon D3100 SLR camera attached to a trinocular Nikon Optiphot equipped with bright-field, dark-field, and phase contrast optics. Images were processed for taking measurements and constructing figures with DVD software, Helicon Focus® software, and CoralPaint®. The map was generated using the open-access mapping Program QGIS (GNU General Public Licence Version 2, June 1991). Map data were provided by the open-access DIVA-GIS system (diva-gis.org), OS OpenData (© Crown copyright, Version: 2022-05; Open Government Licence: https://www.nationalarchives.gov.uk/doc/open-government-licence/version/3/), and OpenStreetMap®, licensed under the Open Data Commons Open Database Licence and the Creative Commons Attribution-ShareAlike 2.0 licence (CC BY-SA 2.0).

After photography, fresh specimens selected for molecular characterisation were washed in filtered seawater and placed in sterile 1.5 ml conical screw-cap microcentrifuge tubes (Fisher Scientific) containing RNA*later*™ (Fisher Scientific). They were then posted to the laboratory in Geneva, where they were photographed with a Leica M205c fitted with a Leica DFC 450C camera before molecular analysis.

Holotypes were usually selected from the same batches as those used for molecular analyses; they were photographed, preserved in isopropyl alcohol, and later transferred to seawater and then 10% buffered formalin (Tables 1 and 2). Paratypes were collected at later dates, photographed, and fixed in 10% formalin or photographed after fixation (Tables 1 and 2). Other specimens were used for molecular characterisation or morphological analysis (Table 1).

2.3. DNA extraction, PCR amplification, and sequencing

DNA was extracted individually from 29 specimens (Table 3; Fig. 3) using guanidine lysis buffer (Holzmann, 2024). Isolate 22044 contains DNA from three specimens that were co-extracted. Semi-nested PCR amplification was carried out for the 18S rDNA barcoding fragment of foraminifera (Pawlowski and Holzmann, 2014) using primers s14F3 (5′-ACG CAM GTG TGA AAC TTG-3′) and sB (5′-TGA TCC TTC TGC AGG TTC ACC TAC-3′) for the first and primers s14F1 (5′-AAG GGC ACC ACA AGA ACG C-3′) and sB for the second amplification. Thirty-five and 25 cycles were performed for the first and the second PCR, with an annealing temperature of 50 °C and 52 °C, respectively. The amplified PCR products were purified using the ROTI® Prep PCR Purification Kit (Roth). Sequencing reactions were performed using the BigDye Terminator v3.1 Cycle Sequencing Kit (Applied Biosystems) and analysed on a 3130XL Genetic Analyser (Applied Biosystems). The resulting sequences were deposited in the NCBI/GenBank database. Isolate and Accession numbers are specified in Table 3 and Figure 3.

2.4. Phylogenetic analysis

The obtained sequences were added to 44 sequences that are part of the publicly available 18S database of monothalamid foraminifera (NCBI/Nucleotide; https://www.ncbi.nlm.nih.gov/nucleotide/). All sequences were aligned using the default parameters of the Muscle automatic alignment option, as implemented in SeaView 4.3.3. (Gouy et al., 2010). The alignment comprises 74 sequences and 1144 sites, all of which were included in the analysis.

The phylogenetic tree (Fig. 3) was constructed using the maximum likelihood method (PhyML 3.0), as implemented in ATGC: PhyML (Guindon et al., 2010). An automatic model selection by SMS (Lefort et al., 2017), based on Akaike Information Criterion (AIC), was used, resulting in a HKY85 + G + I substitution model being selected for the analysis. The initial tree is based on BioNJ. Bootstrap values (BV's) are based on 100 replicates. Pairwise genetic distances have been calculated using Mega 11, with a Maximum Composite Likelihood method and uniform rates among sites applied to the analysis (Kumar et al., 2016).

2.5. ZooBank registration of the present work

This publication was registered in ZooBank with the following code: urn:lsid:zoobank.org:pub:132A7780-72D6-4379-A5DC-FA632A160609.

Table 1.
Details for type specimens and other material.

Taxa	Use and number of specimens	Date	Site	Coordinates
Lorneia sphaerica sp. nov.	***Holotype;*** Molecular (4); Morphology (3)	04/08/2023	Loch Creran (Site 3)	56°30.964′ N, 05°21.614′ W
	Paratypes 1 & 2; Morphology (5)	22/07/2024	Dunstaffnage Bay (Site 4)	56°27.056–130′ N, 05°26.267–315′ W
	Paratypes 3 & 4; Morphology (2)	23/07/2024	Creran Eriska (Site 2)	56°31.518–547′ N, 05°24.387–408′ W
	Morphology (46)	23/07/2024	Creran Eriska (Site 2)	56°31.547′ N, 05°24.387′ W
Lorneia ovalis sp. nov.	***Holotype;*** Morphology (7)	15/11/2023	Creran Eriska (Site 2)	56°31.547′ N, 05°24.387′ W
	Molecular (5); Morphology (9)	28/10/2023	Creran Eriska (Site 2)	56°31.452′ N, 05°24.479′ W
	Paratype 1	23/08/2024	Creran Eriska (Site 2)	56°31.452′ N, 05°24.479′ W
Psammophaga owensi sp. nov.	***Holotype;*** Molecular (6); Morphology (6)	04/08/2023	Loch Creran (Site 3)	56°30.964′ N, 05°21.614′ W
	Morphology (9)	06/08/2023	Dunstaffnage Bay (Site 4)	56°27.107′ N, 05°26.296′ W
	Morphology (4)	06/06/2024	Dunstaffnage Bay (Site 4)	56°27.107′ N, 05°26.303′ W
	Paratypes 1–4; Morphology (8)	22/07/2024	Dunstaffnage Bay (Site 4)	56°27.118′ N, 05°26.296′ W
Hilla brevis sp. nov.	***Holotype;*** Molecular (5); Morphology (4)	06/08/2023	Dunstaffnage Bay (Site 4)	56°27.068′ N, 05°26.280′ W
	Morphology (9)	03/09/2023	Dunstaffnage Bay (Site 4)	56°27.113–142′ N, 05°26.287–299′ W
	Paratypes 1–3	06/06/2024	Dunstaffnage Bay	56°27.107′ N, 05°26.303′ W
	Paratypes 4–7; Morphology (2)	07/06/2024	Creran Eriska (Site 2)	56°31.457–539′ N, 05°24.389–479′ W
	Morphology (7)	23/07/2024	Creran Eriska (Site 2)	56°31.460′ N, 05°24.474′ W
	Morphology (29)	23/07/2024	Creran Eriska (Site 2)	56°31.455′ N, 05°24.477′ W
Flaviatella zaninettiae sp. nov.	***Holotype;*** Molecular (8); Morphology (6)	04/08/2023	Loch Creran (Site 3)	56°30.970′ N, 05°21.667′ W
	Molecular (2)	06/07/2018	Greenland, Nuuk Fjord, Station 16, Inner part of Lysefjord, depth 61 m	64°12.656′ N, 50°15.751′ W
	Molecular (4)	11–13/05/2022	Greenland Sea, Vestnesa seep NW, St. CAGE22–2-KH3/PC8, depth 1400 m	78°02.844′ N, 07°02.400′ E
	Morphology (19)	01/09/2023	Creran Eriska (Site 2)	56°31.550′ N; 05°24.409′ W
	Morphology (1)	28/10/2023	Creran Eriska (Site 2)	56°31.528′ N; 05°24.348′ W
	Paratypes 1–6	07/06/2024	Creran Eriska (Site 2)	56°31.539′ N; 05°24.389′ W
Flexammina islandica	Molecular (1); Morphology (6)	01/09/2023	Creran Eriska (Site 2)	56°31.542′ N; 05°24.220′ W
	Molecular (1); Morphology (3)	03/09/2023	Dunstaffnage Bay (Site 4)	56°27.142′ N; 05°26.299′ W
Ovammina opaca	Molecular (4)	02/09/2023	Loch Laich (Site 1)	56°34.259′ N; 05°23.111′ W
	Morphology (3)	28/10/2023	Creran Eriska (Site 2)	56°31.480′ N; 05°24.570′ W

3. Results

3.1. Taxonomic description

Rhizaria Cavalier-Smith, 2002
Retaria Cavalier-Smith, 1999
Foraminifera d'Orbigny, 1826
Monothalamids Pawlowski et al., 2013

3.1.1. *Lorneia gen. nov. (Monothalamid Clade D)*

Diagnosis. Test free, monothalamous, roughly spherical, diameter 152–551 μm, length/width ratio 1.00–1.37. Minute openings resembling apertures distributed around the test. Surface of test light beige, test wall with 2–12 μm thick organic layer, overlain by variably developed, loosely attached coating of transparent mineral grains of various sizes. Cytoplasm white, opaque, containing mineral grains, including some that are black and magnetic. Concentrations of dark grains discernible through the wall on the underside of the test.

Type species. *Lorneia sphaerica* sp. nov. by original designation (Article 68.2 of the ICZN, 1999).

Etymology. The name is derived from Lorne or Lorn, an ancient province in the west of Scotland and now a district in the Argyll and Bute council area where the new genus was discovered. *Lorneia* is considered feminine (Article 30.2.2 of the ICZN, 1999).

ZooBank registration. The new genus-group name *Lorneia* was registered in ZooBank under the following code: urn:lsid:zoobank.org:act:5FE357F4-2346-4BDD-8DC4-2FE12D98BFCD.

3.1.2. *Lorneia sphaerica sp. nov. (Fig. 4)*

2023 Agglutinated sphere – Henderson, J. Mar. Biol. Assoc. U.K. 103, e18: 13–14, Figs. 9, 10

Diagnosis. As for the genus.

Etymology. The Latin adjective *sphaeric·us*, *-a*, *-um* [m, f, n] (spherical) refers to the spherical shape of the organism.

Zoobank registration. The new species-group name *Lorneia sphaerica* was registered in ZooBank under the following code: urn:lsid:zoobank.org:act:CC1A3922-FE80-4E91-ADBD-E4347DDDDA5F.

Type material (Tables 1 and 2). The type specimens are preserved individually in 10% formalin in 1.5 ml conical screw-cap microcentrifuge tubes (Fisher Scientific) and are deposited in the Natural History Museum, London, under the following registration numbers: Holotype (NHMUK PM ZF 10585) preserved first in isopropyl alcohol and then transferred to 10% formalin, and Paratypes 1–4 (NHMUK PM ZF 10586–10589).

Other material (Table 1). Four specimens for molecular characterisation (isolates 22045–22048) were collected from Site 3, and 56 specimens for morphological analysis from Sites 2, 3, and 4. Also included are descriptions and measurements of 270 specimens collected in 2020–2021, which featured in Henderson (2023).

Description based on all material from 2020–2021 and 2023–2024. The test is spherical or slightly spheroidal (Fig. 4) with the following dimensions (n = 335): length 297 ± 67 μm (range 155–551 μm), width 279 ± 66 μm (range 152–534 μm), and length/width ratio 1.07 ± 0.07 (range 1.00–1.37). The individual dimensions for the holotype and four paratypes are given in Table 2. There are several minute apertures distributed around the test wall, only visible under high-power bright-field in tests embedded in glycerol (Henderson, 2023).

The basic test wall is transparent, 2–12 μm thick (n = 31), and composed of organic material. It is overlain by a variably developed layer of loosely agglutinated, relatively coarse, multicoloured mineral particles mixed with fine sediment so that the surface appears light beige (Fig. 4A). Although the amount of agglutinated material varies between individuals, there are no clearly demarcated subtypes. The four paratypes were selected as representatives of different degrees of agglutination (Fig. 4C); the transparent organic test wall is discernible in Paratype 4, which has the least agglutination.

The cytoplasm is white, opaque, and contains ingested mineral particles, some of which are black and probably magnetite, as the species is magnetic. A concentration of the dark grains is often visible through the wall on the underside of the test as it rests on a substrate, reflecting their high density.

In sediment that has been settled in Petri dishes, the tests occupy a subsurface microhabitat and are therefore not visible under a stereomicroscope, although they can be extracted in large numbers by a magnet. Once the specimens are released upon a glass slide, they deploy granulo-reticulopodia from several points around the test wall, most likely from the small, simple apertures noted above (Henderson, 2023).

Comparison between 2020–2021 and 2023–2024 material. This previously unnamed species was described in some detail as an 'Agglutinated sphere' by Henderson (2023). It was observed in great abundance in the autumn of 2020 and 2021 in Dunstaffnage Bay. In the 2023–2024 material, only a few were seen at the same sampling spots in Dunstaffnage Bay, but specimens were also found in moderate numbers in the two Loch Creran habitats (Sites 2 and 3). The 2020–2021 specimens described by Henderson (2023) from Dunstaffnage Bay were significantly larger ($p < 0.05$, t-test) than the 2023–2024 cohort and had the following dimensions (n = 270): length 313 ± 64 μm (range 155–551 μm), width 294 ± 64 μm (range 152–534 μm), and length/width ratio 1.07 ± 0.07 (range 1.00–1.37). The 2023–2024 group had the following dimensions (n = 65): length 232 ± 29 μm (range 175–315 μm), width 219 ± 30 μm (range 154–315 μm), and length/width ratio 1.06 ± 0.05 (range 1.00–1.26). Otherwise, specimens from the two sampling periods had similar characteristics. In both cases, they were spherical or nearly spherical (spheroidal) with intracellular magnetic particles that tend to collect at the lowest point, and a test wall with a loosely agglutinated veneer, the same colour as the sediment.

Molecular characteristics. *Lorneia sphaerica* monothalamids form a well-supported group (97% BV) that branches in Clade D as sister to *Hippocrepinella hirudinea* Heron-Allen & Earland, 1932 and *Hippocrepinella* sp., albeit without support (Table 3; Fig. 3). The partial SSU rDNA sequences of *L. sphaerica* contain 896 nucleotides, and the GC content is 43%. Pairwise sequence distance mounts from 0 to 0.003.

Remarks. The ingestion of magnetic particles is an interesting feature of the new species. Some of the *Psammophaga* species, for

Table 2.
Dimensions of type specimens.

Taxa	Type	Length (in μm)	Width (in μm)	L/W
Lorneia sphaerica	*Holotype*	260	252	1.03
	Paratype 1	264	242	1.09
	Paratype 2	291	273	1.07
	Paratype 3	282	273	1.03
	Paratype 4	285	273	1.04
Lorneia ovalis	*Holotype*	588	353	1.67
	Paratype 1	570	350	1.63
Psammophaga owensi	*Holotype*	421	238	1.77
	Paratype 1	579	268	2.16
	Paratype 2	563	295	1.91
	Paratype 3	589	263	2.24
	Paratype 4	589	289	2.04
Hilla brevis	*Holotype*	508	373	1.36
	Paratype 1	719	479	1.50
	Paratype 2	591	395	1.49
	Paratype 3	555	418	1.33
	Paratype 4	736	537	1.37
	Paratype 5	523	477	1.10
	Paratype 6	702	537	1.31
	Paratype 7	536	464	1.16
Flaviatella zaninettiae	*Holotype*	906	378	2.40
	Paratype 1	739	261	2.83
	Paratype 2	652	217	3.00
	Paratype 3	583	191	3.05
	Paratype 4	652	287	2.27
	Paratype 5	635	278	2.28
	Paratype 6	983	287	3.42

Table 3.
Data for molecularly characterised specimens and comparisons with similar species.

Species/Clade	Isolate	Accession number	Sampling location
Clade M			
Flexammina islandica	17667	KM097044	Iceland
Flexammina islandica	17678	KM097064	Iceland
Flexammina islandica	**22118**	**PV072533**	**Scotland, Eriska, Site 2, 56°31.542' N, 05°24.220' W**
Flexammina islandica	**22119**	**PV072534**	**Scotland, Dunstaffnage Bay, Site 4, 56°27.142' N, 05°26.299' W**
Clade E			
Psammophaga owensi	**22041**	**PV072525**	**Scotland, Loch Creran, Site 3, 56°30.964' N, 05°21.614' W**
Psammophaga owensi	**22042**	**PV072526**	**Scotland, Loch Creran, Site 3, 56°30.964' N, 05°21.614' W**
Psammophaga owensi	**22043**	**PV072527**	**Scotland, Loch Creran, Site 3, 56°30.964' N, 05°21.614' W**
Psammophaga owensi	**22044**	**PV072528**	**Scotland, Loch Creran, Site 3, 56°30.964' N, 05°21.614' W**
Psammophaga fuegia	17392	KU313692	Chile, Beagle Channel
Psammophaga fuegia	17510	KU313694	Chile, Beagle Channel
Psammophaga magnetica	2976	FN995274	Antarctica, Mc Murdo Sound
Psammophaga magnetica	3184	FN995272	Antarctica, Mc Murdo Sound
Psammophaga secriensia	9486	OQ845891	Black Sea, Balaclava Bay
Psammophaga secriensia	21480	OQ845894	Black Sea, Romanian continental Shelf
Psammophaga sp.	12297*	PQ184287, PQ184288	Denmark, Aarhus Bay
Psammophaga sp.	12312*	PQ184295, PQ184296	Denmark, Aarhus Bay
Psammophaga sp.	16356*	PQ184276, PQ184277	Scotland, Dunstaffnage Bay
Psammophaga zirconia	9495	LN886765	Black Sea, Omega Bay
Psammophaga zirconia	18412	LN886768	Italy, Adriatic Sea
Clade O			
Cedhagenia saltatus	10141	FN995339	Black Sea, Balaclava Bay
Cedhagenia saltatus	10149	FN995343	Black Sea, Balaclava Bay
Ovammina opaca	2399	OR918359	Denmark, Nissum Bredning
Ovammina opaca	2485	AJ307755	Barents Sea
Ovammina opaca	**22103**	**PV072529**	**Scotland, Loch Laich, Site 1, 56°34.259' N, 05°23.111' W**
Ovammina opaca	**22104**	**PV072530**	**Scotland, Loch Laich, Site 1, 56°34.259' N, 05°23.111' W**
Ovammina opaca	**22105**	**PV072531**	**Scotland, Loch Laich, Site 1, 56°34.259' N, 05°23.111' W**
Ovammina opaca	**22106**	**PV072532**	**Scotland, Loch Laich, Site 1, 56°34.259' N, 05°23.111' W**
Clade Y			
Flaviatella profunda	9296	OR428499	Pacific, Japan Trench
Flaviatella profunda	21797	OR428525	Pacific, Aleutian Trench
Flaviatella profunda	21798	OR428526	Pacific, Aleutian Trench
Flaviatella siemensma	21385	OM422876	East Falkland, Port William
Flaviatella siemensma	21387	OM422877	East Falkland, Port William
Flaviatella siemensma	21388	OM422878	East Falkland, Port William
Flaviatella zaninettiae	**22033**	**PV072547**	**Scotland, Loch Creran, Site 3, 56°30.970' N, 05°21.667' W**
Flaviatella zaninettiae	**22034**	**PV072548**	**Scotland, Loch Creran, Site 3, 56°30.970' N, 05°21.667' W**
Flaviatella zaninettiae	**22035**	**PV072549**	**Scotland, Loch Creran, Site 3, 56°30.970' N, 05°21.667′ W**
Flaviatella zaninettiae	**22036**	**PV072550**	**Scotland, Loch Creran, Site 3, 56°30.970' N, 05°21.667' W**
Flaviatella zaninettiae	**22037**	**PV072551**	**Scotland, Loch Creran, Site 3, 56°30.970' N, 05°21.667' W**
Flaviatella zaninettiae	**22038**	**PV072552**	**Scotland, Loch Creran, Site 3, 56°30.970' N, 05°21.667' W**
Flaviatella zaninettiae	**22039**	**PV072553**	**Scotland, Loch Creran, Site 3, 56°30.970' N, 05°21.667' W**
Flaviatella zaninettiae	**22040**	**PV072554**	**Scotland, Loch Creran, Site 3, 56°30.970' N, 05°21.667' W**
Flaviatella zaninettiae	**20348**	**ON550607**	**Greenland, Nuuk Fjord, 64°12.656' N, 50°15.751' W**
Flaviatella zaninettiae	**20350**	**ON550608**	**Greenland, Nuuk Fjord, 64°12.656' N, 50°15.751' W**
Flaviatella zaninettiae	**21699**	**OQ883888**	**Greenland Sea, Vestnesa seep NW, 78°02.844' N, 07°02.400′ E**
Flaviatella zaninettiae	**21700**	**OQ883889**	**Greenland Sea, Vestnesa seep NW, 78°02.844′ N, 07°02.400′ E**
Flaviatella zaninettiae	**21701**	**OQ883890**	**Greenland Sea, Vestnesa seep NW, 78°02.844' N, 07°02.400′ E**
Flaviatella zaninettiae	**21702**	**OQ883891**	**Greenland Sea, Vestnesa seep NW, 78°02.844' N, 07°02.400′ E**
Hilla brevis	**22049**	**PV072544**	**Scotland, Dunstaffnage Bay, Site 4, 56°27.068' N, 05°26.280' W**
Hilla brevis	**22050**	**PV072545**	**Scotland, Dunstaffnage Bay, Site 4, 56°27.068′ N, 05°26.280′ W**
Hilla brevis	**22051**	**PV072546**	**Scotland, Dunstaffnage Bay, Site 4, 56°27.068' N, 05°26.280′ W**
Hilla arctica	21703	OQ883882	Svalbard, Vestnesa Ridge
Hilla arctica	21704	OQ883883	Svalbard, Vestnesa Ridge
Hilla argentea	21335	OM422873	South Georgia Island, Cumberland Bay
Hilla argentea	21336	OM422874	South Georgia Island, Cumberland Bay
Nujappikia idaliae	19842	ON053404	Greenland, Nuuk Fjord
Nujappikia idaliae	19847	ON053407	Greenland, Nuuk Fjord
Clade D			
Hippocrepinella hirudinea	21241	OM422931	South Georgia Island, Fortuna Bay
Hippocrepinella hirudinea	21242	OM422932	South Georgia Island, Fortuna Bay
Hippocrepinella sp.	18576*	OL772077, OL772078	Pacific deep sea, Clarion-Clipperton Zone
Hippocrepinella sp.	20266	ON053394	Greenland, Nuuk Fjord
Hippocrepinella sp.	20267	ON053396	Greenland, Nuuk Fjord
Lorneia sphaerica	**22045**	**PV072535**	**Scotland, Loch Creran, Site 3, 56°30.964' N, 05°21.614' W**
Lorneia sphaerica	**22046**	**PV072536**	**Scotland, Loch Creran, Site 3, 56°30.964' N, 05°21.614' W**
Lorneia sphaerica	**22047**	**PV072537**	**Scotland, Loch Creran, Site 3, 56°30.964' N, 05° 21.614' W**
Lorneia sphaerica	**22048**	**PV072538**	**Scotland, Loch Creran, Site 3, 56°30.964' N, 05°21.614' W**
Lorneia ovalis	**22179**	**PV072539**	**Scotland, Eriska, Site 2, 56°31.452' N, 05°24.479' W**
Lorneia ovalis	**22180**	**PV072540**	**Scotland, Eriska, Site 2, 56°31.452' N, 05°24.479' W**
Lorneia ovalis	**22181**	**PV072541**	**Scotland, Eriska, Site 2, 56°31.452' N, 05°24.479' W**
Lorneia ovalis	**22182**	**PV072542**	**Scotland, Eriska, Site 2, 56°31.452' N, 05°24.479' W**
Lorneia ovalis	**22183**	**PV072543**	**Scotland, Eriska, Site 2, 56°31.452' N, 05°24.479' W**

Specimens marked in bold have been investigated for the present study.
* PCR products have been cloned prior to sequencing.

example, *P. magnetica* Pawlowski and Majewski, 2011 from Admiralty Bay, West Antarctica (Pawlowski and Majewski, 2011) and *P. zirconia* Sabbatini, Bartolini & Morigi, 2016 from the Adriatic Sea (Sabbatini et al., 2016), are also often magnetic, as is the hadal species *Resigella bilocularis* Gooday, Todo, Uematsu & Kitazato, 2008 Gooday et al., 2008; Yang et al., 2022). Some foraminifera seem to have an affinity for heavy minerals, and so these species are not necessarily attracted to the magnetic properties of the grains, but rather to their high density.

The placement of a new genus in Clade D indicates a distant relationship with the genus *Hippocrepinella*, notably *H. hirudinea* and other closely related members of this genus, found in sublittoral and deeper water settings from various parts of the world (Gooday et al., 2022; Heron-Allen and Earland, 1932; Himmighofen et al., 2023; Holzmann et al., 2022; Pawlowski et al., 2008). However, *Hippocrepinella* species are characterised by an elongate, basically tubular test open at both ends, and are considerably larger than the new species. Agglutinated foraminifera with spherical tests are often assigned to the genus *Psammosphaera* based on morphological criteria, but members of

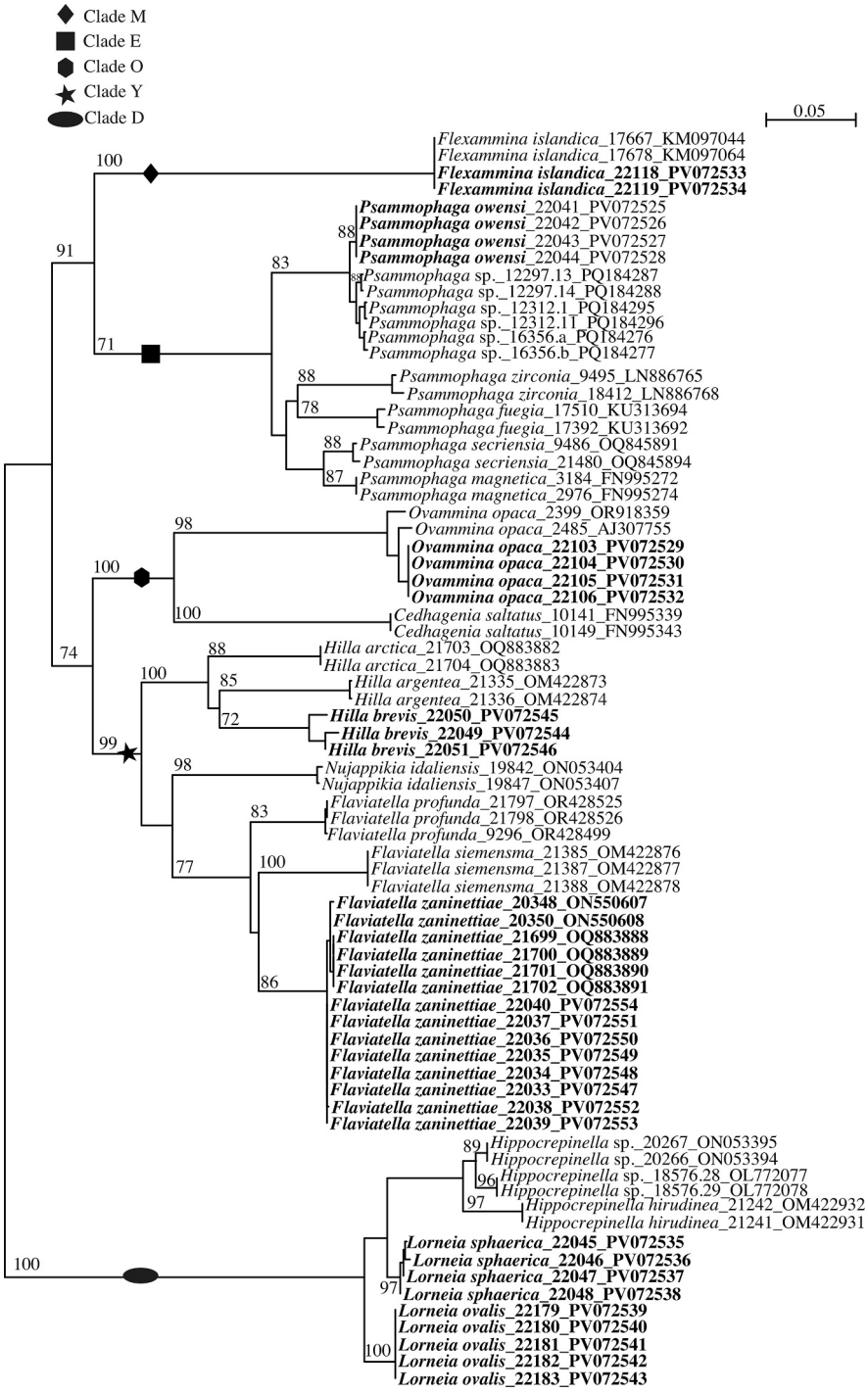

Fig. 3. PhyML phylogenetic tree based on the 3′ end fragment of the SSU rRNA gene, showing the evolutionary relationships of 74 monothalamid foraminiferal sequences belonging to Clades M, E, O, Y, and D (Pawlowski et al., 2002, 2013, 2014). Taxa in bold are those which feature in the present study. The tree is unrooted. Specimens are identified by their isolate numbers followed by their accession numbers (2nd). Numbers at the nodes refer to bootstrap values that are greater than 70%.

this genus are much larger and more robust. Tiny agglutinated spheres from the abyssal Clarion-Clipperton Zone are more similar in general appearance to the new species (Gooday and Goineau, 2019; Ohkawara et al., 2009) but are even smaller with different kinds of wall structure and interiors dominated by stercomata (waste pellets).

3.1.3. *Lorneia ovalis sp. nov.* (Fig. 5)

Diagnosis. Test free, monothalamous, oval with rounded or flattened ends, length 354–772 μm, width 276–457 μm, length/width ratio 1.22–2.00. Terminal aperture structures located at each end of the test. Surface of test light beige with 10 μm thick organic layer overlain by coarse, multi-coloured grains; in live specimens, the test is embedded in a thick mass of sediment. Cytoplasm densely packed with mineral particles, many of which are black and magnetic.

Etymology. The Latin adjective *oval·is*, *-is*, *-e* [m, f, n] (oval, egg-shaped) refers to the oval shape of the organism.

Zoobank registration. The new species-group name *Lorneia ovalis* was registered in ZooBank under the following code: urn:lsid:zoobank.org:act:BF18F0B7-01A5-4193-9CB3-88FD13A4CE45.

Type material (Tables 1 and 2). The type specimens are preserved individually in 10% formalin in 1.5 ml conical screw-cap microcentrifuge tubes (Fisher Scientific) and are deposited in the Natural History Museum, London, under the following registration numbers: Holotype (NHMUK PM ZF 10590) initially preserved in isopropyl alcohol, then transferred to 10% formalin, and Paratype 1 (NHMUK PM ZF 10591).

Other material (Table 1). Five specimens for molecular characterisation (isolates 22179–22183) were collected from Site 2, and 16 specimens for morphological analysis from Site 2.

Description. The test is quite variable in shape and size (Fig. 5) but generally oval with rounded or flattened ends and the following dimensions (n = 23): length 546 ± 107 μm (range 354–772 μm), width 353 ± 51 μm (range 276–457 μm), and length/width ratio 1.55 ± 0.24 (range 1.22–2.00). The dimensions of the holotype and paratype (Fig. 5E, F) are given in Table 2. In live specimens, sparse pseudopodia emerge from terminal aperture structures that are partly obscured by agglutinated material and often difficult to see in transmitted light. In some, capsule-like apertural structures project slightly from the ends of the test, while in others, the apertures seem to be associated with shallow concave depressions of the test wall (Fig. 5A–D).

The test wall comprises a single layer of transparent organic material, 10 μm thick, overlain and largely obscured by coarse, multi-coloured agglutinated grains interspersed with sediment so that in reflected light the test has a grey or light-beige surface. The cytoplasm is filled with a dense concentration of dark mineral grains that are discernible through the test wall.

In sediment settled in Petri dishes, the tests are buried under the surface of the sediment and typically embedded in a ball of fine, muddy sediment. This, together with the test agglutination and infaunal microhabitat, ensures that they are not visible under a

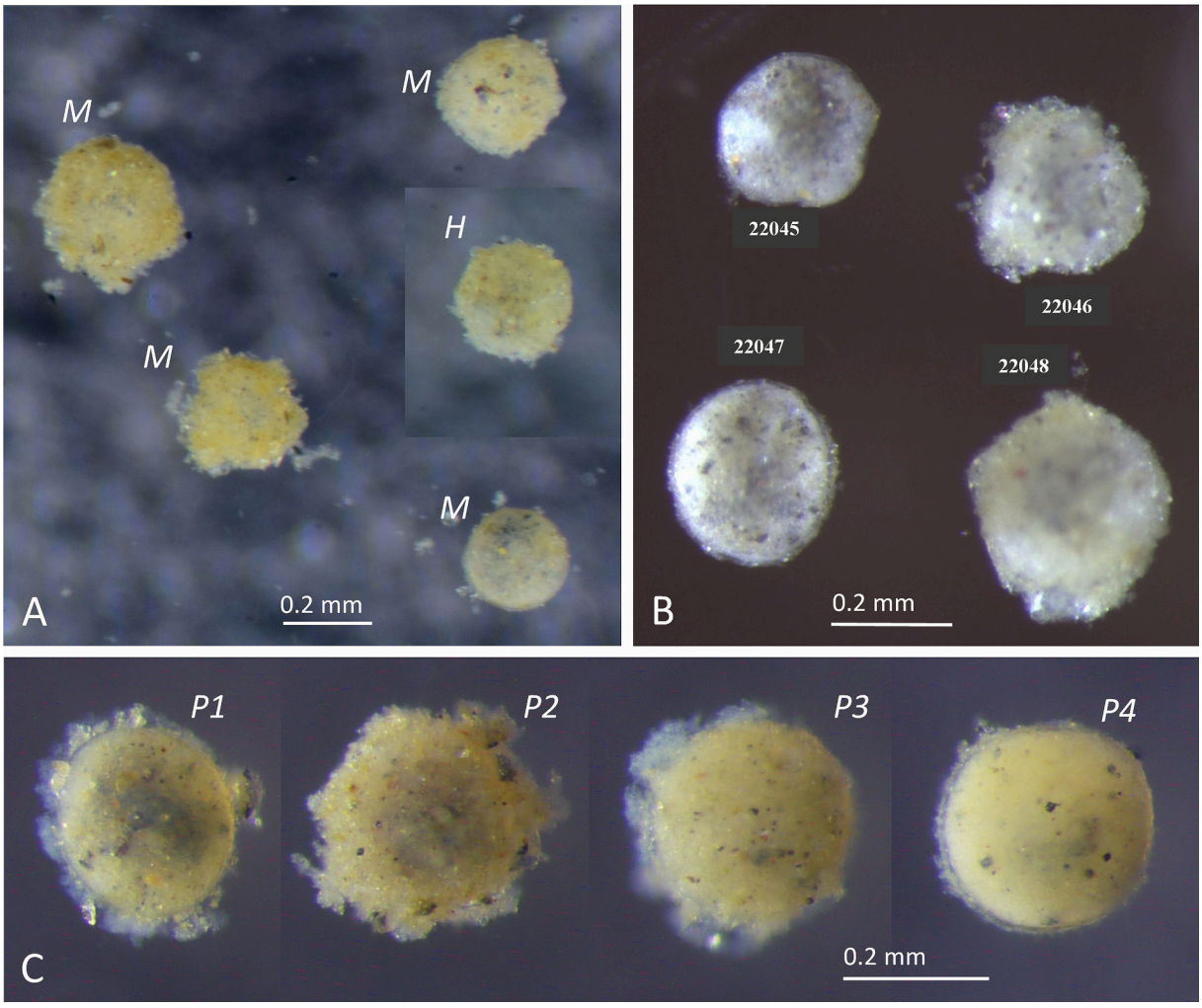

Fig. 4. *Lorneia sphaerica* gen. & sp. nov. (**A**) Fresh specimens (*M* = destined for molecular determination; *H* = holotype). (**B**) The specimens labelled "M" now in RNA*later*™; their numbers correspond to subsequently extracted isolates. (**C**) Paratypes *P1–P4* (fresh material).

stereomicroscope. However, specimens can be extracted with a magnet. Removal of the mud coating with a pair of fine brushes exposes the underlying test with its coarsely agglutinated outer layer. The coarse grains are loosely attached and can also be removed with fine brushes, revealing the transparent layer and the dark particles within the cell.

Molecular characteristics. *Lorneia ovalis* forms a strongly supported group (100% BV) that branches in Clade D at the base of *L. sphaerica*, *H. hirudinea*, and *Hippocrepinella* sp. (Fig. 3). The partial SSU rDNA sequences of *L. sphaerica* contain 896 nucleotides, and the GC content is 43%. The five obtained sequences are identical.

Remarks. Most of the specimens, including the types, were collected from a very localised area on the beach in Loch Creran near Eriska Island (Site 2) in late October 2023 (Tables 1 and 2). Ten were used for genetic analysis, of which five gave positive results. During the following month, fewer specimens were found. Except for one specimen, they were not seen at the same site at any time during 2024. In order to identify this

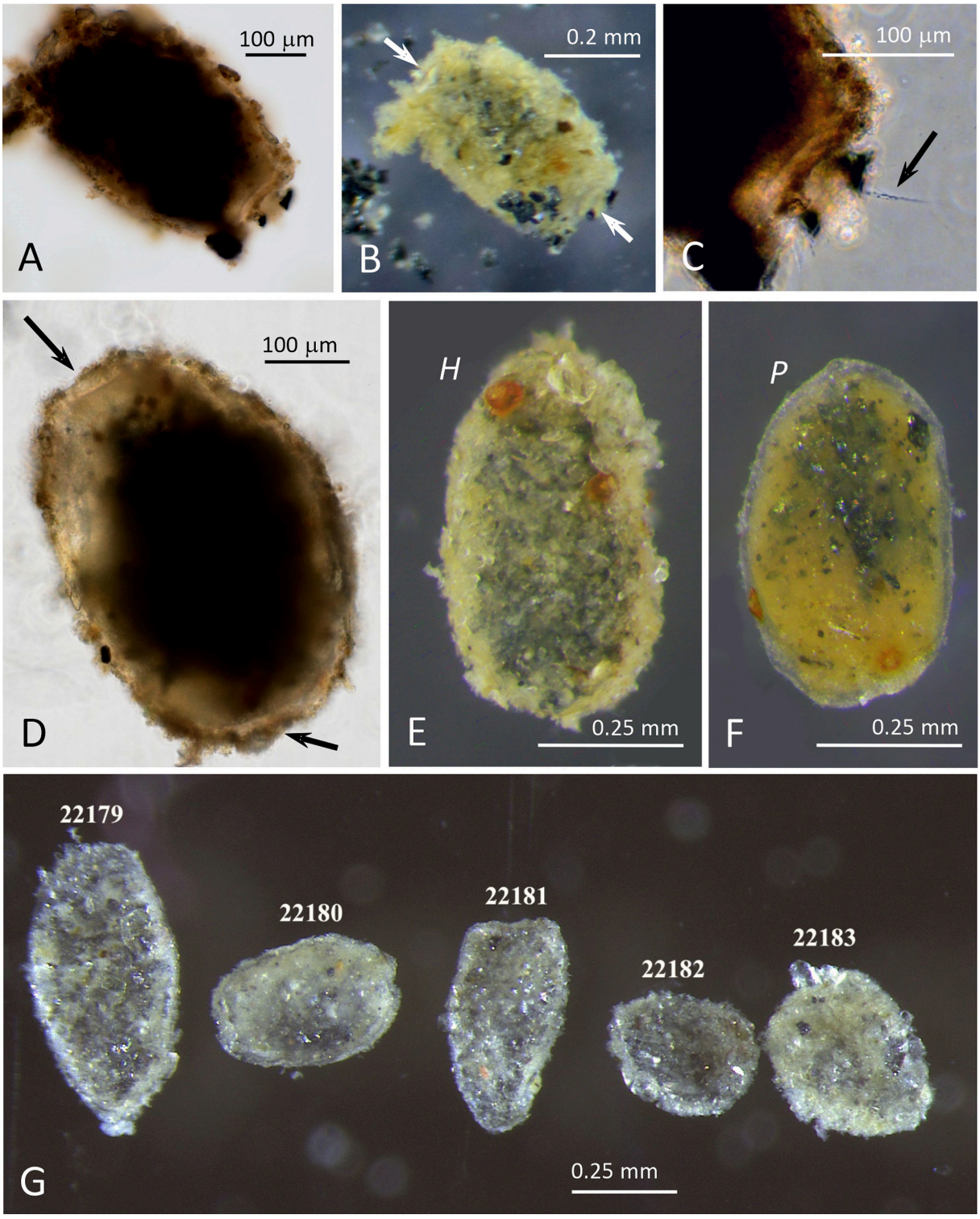

Fig. 5. *Lorneia ovalis* gen. & sp. nov. (**A–D**) Fresh specimens (apertures arrowed) under transmitted and reflected lighting. (**E, F**) Specimens in 10% formalin (*H* = holotype; *P* = paratype). (**G**) Specimens destined for molecular determination in RNA*later*™; their numbers correspond to subsequently extracted isolates.

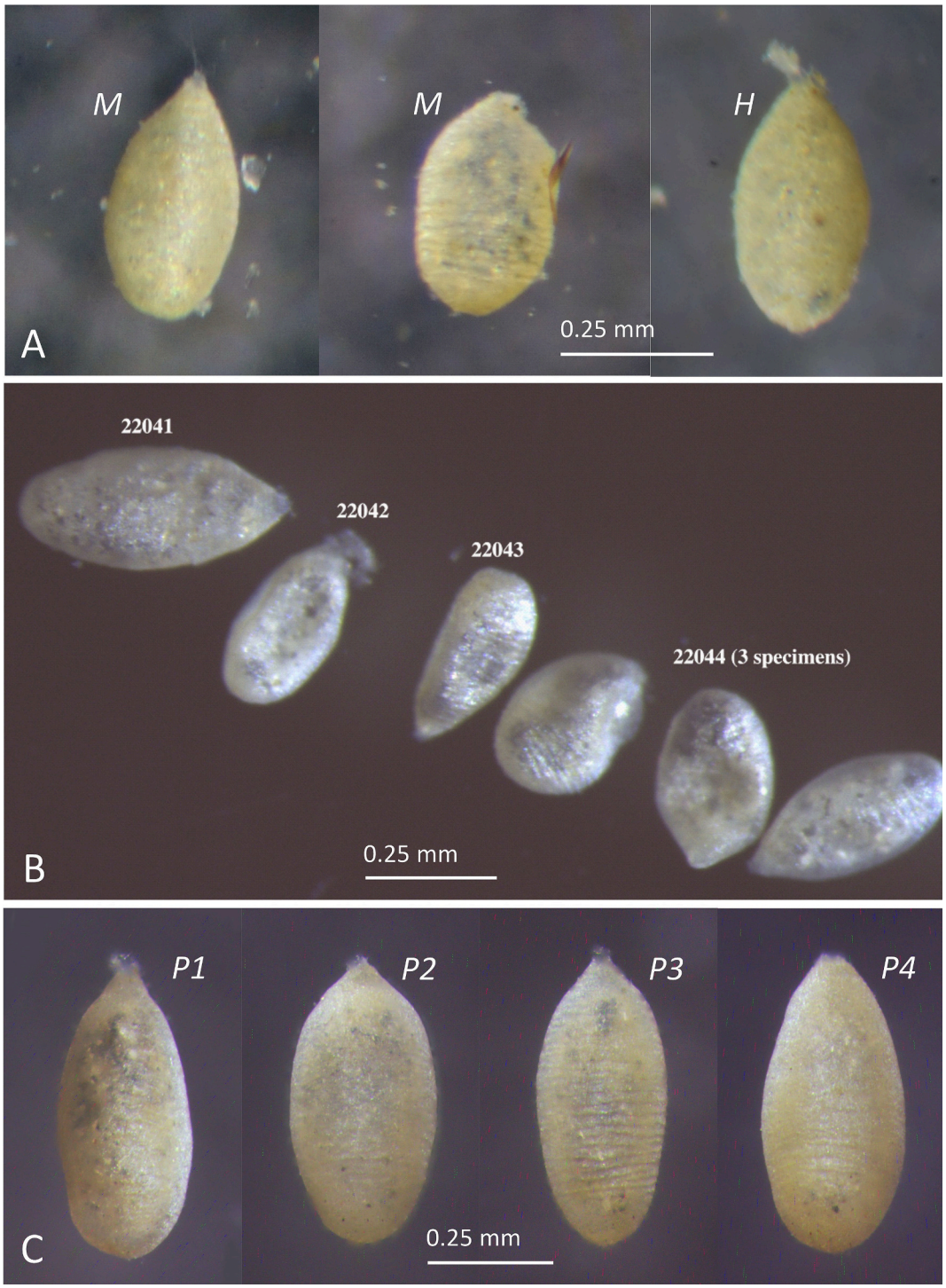

Fig. 6. *Psammophaga owensi* sp. nov. (**A**) Fresh specimens (*M* = destined for molecular determination; *H* = holotype). (**B**) Specimens for destined molecular determination in RNA*later*™; their numbers correspond to subsequently extracted isolates. (**C**) Paratypes *P1–P4* (fresh material).

species, it is important to remove the fine sediment coating (cyst) that obscures live specimens because similar cyst-like structures may enclose other monothalamids.

Lorneia ovalis is closely related to *L. sphaerica* but is elongate rather than spherical, with two terminal apertures rather than multiple apertures dispersed across the test. It is more distantly related to *Hippocrepinella* and completely different morphologically (Gooday et al., 2022; Himmighofen et al., 2023; Holzmann et al., 2022). *Psammophaga* also accumulates dark mineral grains, and some species are magnetic. However, species of this genus have a single aperture and a very finely agglutinated test surface, as well as being located genetically in Clade E.

3.1.4. *Psammophaga owensi sp. nov. (Monothalamid Clade E)* (*Fig. 6*)

2023 *Psammophaga* sp. – Henderson, J. Mar. Biol. Assoc. U.K. 103, e18: 7–9, Figs. 3F–G and 4

Diagnosis. Test free, monothalamous, oval with a more or less pointed apertural end, length 218–643 µm, width 112–329 µm, length/width ratio 1.27–2.63. Terminal aperture structure simple and cone-shaped. Surface of test light beige or grey, reflective, smooth or with transverse ridges. Test wall 2–12 µm thick, composed of organic

material overlain with a finely agglutinated veneer. Cytoplasm white, opaque; contains mineral grains, including black and magnetic ones. Concentrations of dark grains discernible through the test wall on the underside of the cell. No peduncle visible.

Etymology. Named in honour of Professor Nicholas J.P. Owens, director of the Scottish Association for Marine Science. Without his support, this project would not have been possible.

Zoobank registration. The new species-group name *Psammophaga owensi* was registered in ZooBank under the following code: urn:lsid:zoobank.org:act:09153122-58B1-4BDD-863B-18FCFEB14B9D.

Type material (Tables 1 and 2). The type specimens are preserved individually in 10% formalin in 1.5 ml conical screw-cap micro-centrifuge tubes (Fisher Scientific) and are deposited in the Natural History Museum, London, under the following registration numbers: Holotype (NHMUK PM ZF 10592) was preserved in isopropyl alcohol and then transferred to 10% formalin, and Paratypes 1–4 (NHMUK PM ZF 10593–10596).

Other material (Table 1). Six specimens for molecular characterisation (isolates 22041–22044) were collected from Site 3, and 27 specimens for morphological analysis from Sites 3 and 4. The descriptions also include 124 specimens collected in 2020–2021, which featured in Henderson (2023).

Description based on all material from 2020–2021 and 2023–2024. The test has an elongate ovate shape with a pointed apertural end and a rounded abapertural end (Fig. 6). The dimensions are (n = 162): length 437 ± 70 µm (range 218–643 µm), width 245 ± 32 µm (range 112–329 µm), and length/width ratio 1.79 ± 0.26 (range 1.27–2.63). Individual dimensions for the holotype (Fig. 6A) and four paratypes (Fig. 6C) are given in Table 2. The test wall is pliable; it can be easily dented and often deforms with handling or when placed in alcohol or RNA*later*™ (Fig. 6B). It is translucent and comprises an outer veneer, 2–9 µm thick, of fine, mostly transparent mineral grains, overlying an organic layer that is 3–9 µm thick (n = 22). In reflected light, the test has a light grey surface with a reflective sheen, and possesses transverse ridges with various degrees of prominence, best seen in oblique incident lighting (Fig. 6C). The apertural structure is a simple cone that forms an extension of the shape of the test, and ranges from blunt to more elongated. The cytoplasm is white and opaque, and concentrations of dark mineral grains within the cytoplasm are discernible through the test wall in glycerol-embedded specimens, either on the underside of the test or congregated at either one end or the other (Fig. 4 in Henderson, 2023). The holotype and four paratypes were selected as representatives of different degrees of ridging on the test surface and variation in the acute angle of the aperture structure (Fig. 6C).

In sediment settled in Petri dishes, the tests lie buried under the surface and are difficult to spot under a stereomicroscope, but they can be extracted in large numbers by a magnet. Once the specimens are released onto a glass slide, they produce a rather sparse set of granulo-reticulopodia that issue from the terminal aperture.

Comparison between 2020–2021 and 2023–2024 material. This species is ubiquitous at the sampling sites and was recovered at different times of the year in 2020–2021 and 2023–2024. The dimensions for the earlier collected specimens were as follows (n = 124): length 425 ± 61 µm (range 218–597 µm), width 244 ± 32 µm (range 112–323 µm), and length/width ratio 1.76 ± 0.24 (range 1.27–2.34). They were significantly smaller ($p < 0.005$, t-test) than the later cohort, which had the following dimensions (n = 38): length 473 ± 83 µm (range 349–643 µm), width 252 ± 30 µm (range 198–329 µm), and length/width ratio 1.89 ± 0.31 (range 1.41–2.63).

Molecular characteristics. *Psammophaga owensi* (88% BV) forms a

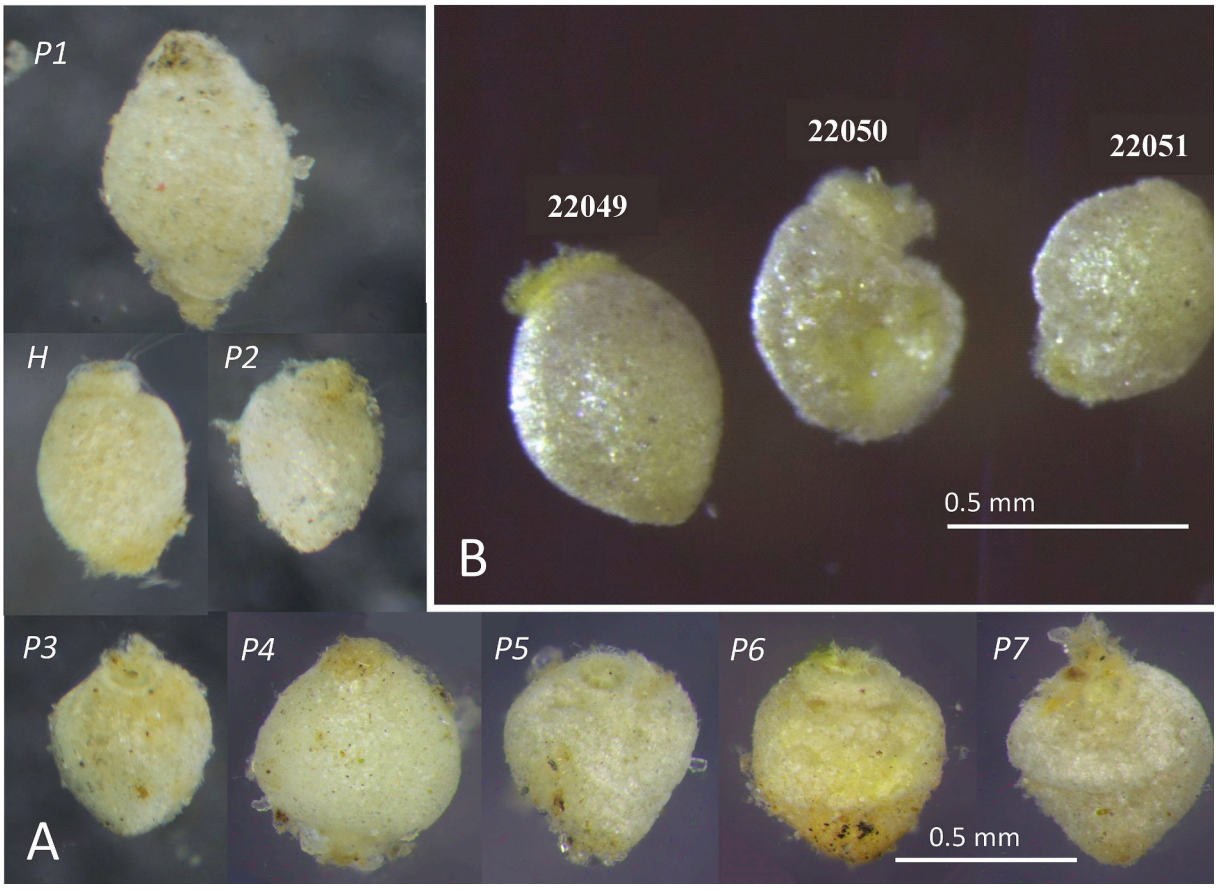

Fig. 7. *Hilla brevis* sp. nov. (**A**) Fresh specimens (H = holotype; $P1$–$P7$ = paratypes). (**B**) Specimens destined for molecular determination in RNA*later*™; their numbers correspond to subsequently extracted isolates.

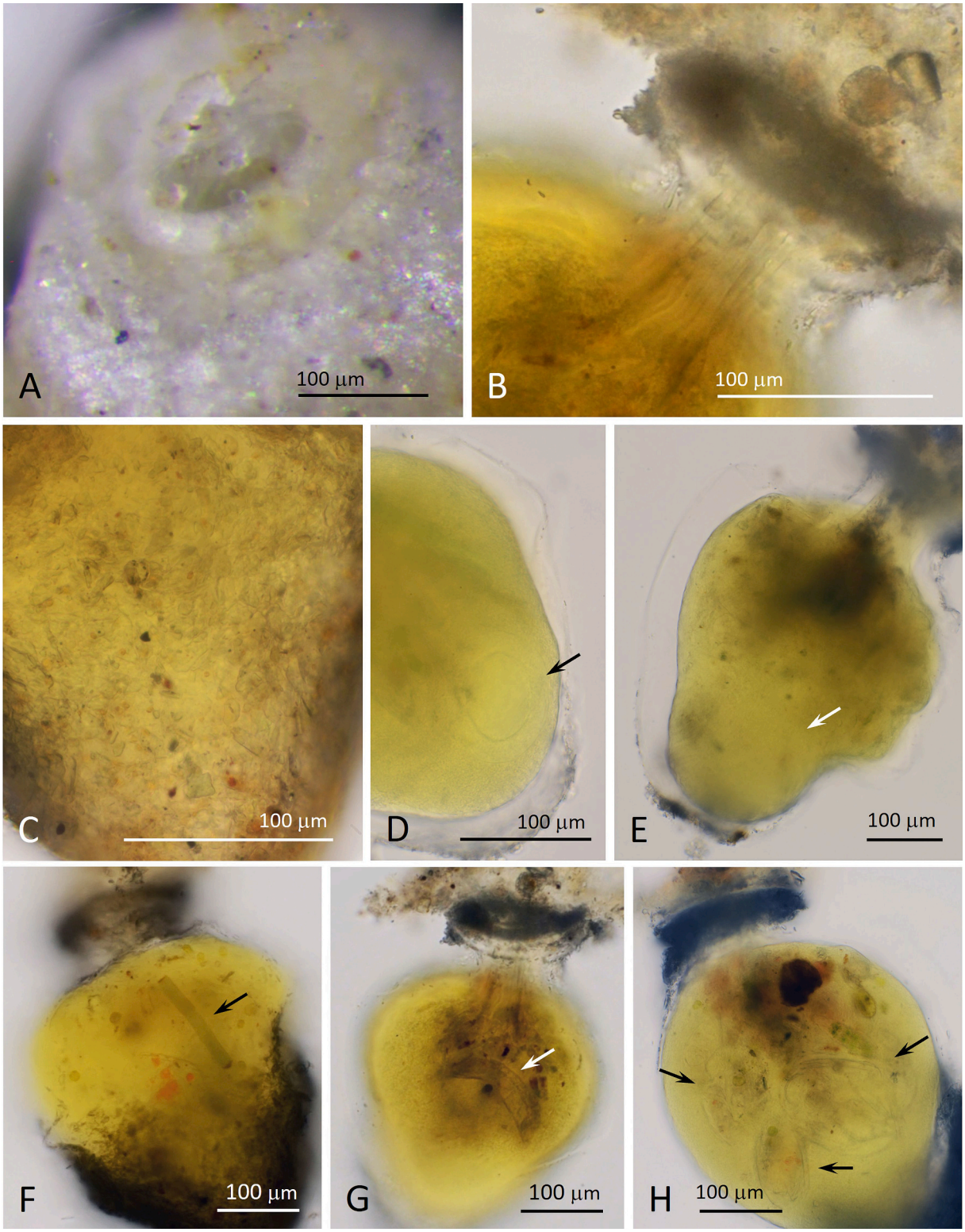

Fig. 8. *Hilla brevis* sp. nov. (**A**) Top view of the apertural structure in a fresh specimen. (**B–H**) Formalin-fixed specimens embedded in glycerol (the test wall agglutination has mostly sloughed off revealing the contents of the cytoplasm). (**B**) Apertural collar. (**C**) Surface view of agglutination of a section of intact test wall. (**D**) Nucleus (arrowed) and transparent organic test wall. (**E**) Nucleus (arrowed), organic test wall and accumulation of ingested material under the aperture structure. (**F**) Ingested cyanobacterial filament (arrowed). (**G**) Ingested diatom frustule (arrowed). (**H**) Large ingested food items (arrowed).

strongly supported group (83% BV) with *Psammophaga* sp. collected from Aarhus Bay and Dunstaffnage Bay (Table 3; Fig. 3). The partial SSU rDNA sequences of *P. owensi* contain 973 nucleotides, and the GC content is 47%. The four obtained sequences are identical.

Remarks. The new species joins ten previously described *Psammophaga* species distributed worldwide and listed in the World Register of Marine Species. All are very much alike in morphology, and some are magnetic, but it is unknown whether this feature reflects the ambient

substratum or is a species-specific characteristic. Those species that have emerged since publication of the earlier paper (Henderson, 2023) are *Psammophaga secriensia* (Fig. 5 in Pavel et al., 2023), sampled at depths of 5–53 m off the northwestern coast of the Black Sea, *Psammophaga holzmannae* (Fig. 2 in Kaushik et al., 2024), and *Psammophaga sinhai* (Fig. 5 in Kaushik et al., 2024) from tropical intertidal sites on the west coast of India.

Psammophaga sequences cluster together in Clade E, which also includes the marine genera *Vellaria*, *Niveus*, *Nellya*, and the freshwater genus *Poseidonella* (Holzmann and Siemensma, 2025; Pawlowski et al., 2002, 2013; Voltski and Pawlowski, 2015). Six publications feature phylogenetic trees that include described and undescribed species of *Psammophaga* from different parts of the world (Gooday et al., 2011; Gschwend et al., 2016; Pavel et al., 2023; Pawlowski and Majewski, 2011; Pawlowski et al., 2008; Sabbatini et al., 2016). The species examined in the current study is closely related to isolate 16356 from Scotland, Dunstaffnage Bay, and isolates 12297 and 12312 from Aarhus Bay, Denmark (Table 3; Fig. 3).

3.1.5. *Hilla brevis sp. nov. (Monothalamid Clade Y) (Figs. 7 and 8)*

Diagnosis. Test free, monothalamous, broadly oval or fusiform in shape, length 350–736 μm, width 224–595 μm, length/width ratio 1.00–2.00. Relatively large terminal aperture surrounded by a pronounced collar. Surface of test white or cream with reflective sheen. Wall with organic layer, 18–25 μm thick, overlain by finely agglutinated coating. Cytoplasm opaque, white, but turning lemon yellow in formalin or RNA*later*™ solutions; contains ingested prey, including diatom frustules and cyanobacterial filaments. Mineral grains absent. No peduncle visible.

Etymology. The Latin adjective *brev·is*, *-is*, *-e* [m, f, n] (short, small, little, narrow) refers to the small length/width ratio, as other known members of this genus are typically elongated.

Zoobank registration. The new species-group name *Hilla brevis* was registered in ZooBank under the following code: urn:lsid:zoobank.org:act:920B3511-31E6-4074-BA4F-66BBC43BA8EB.

Type material (Tables 1 and 2). The type specimens are preserved individually in 10% formalin in 1.5 ml conical screw-cap microcentrifuge tubes (Fisher Scientific) and are deposited in the Natural History Museum, London, under the following registration numbers: Holotype (NHMUK PM ZF 10597) preserved first in isopropyl alcohol and then transferred to 10% formalin, and Paratypes 1–7 (NHMUK PM ZF 10598–10604).

Other material (Table 1). Five specimens for molecular characterisation (isolates 22049–22051) were collected from Site 4, and 51 specimens for morphological analysis from Sites 2 and 4.

Description. The test is free, monothalamous and broadly ovate with a somewhat truncated apertural end and a rounded or pointed abapertural end (Fig. 7). It has the following dimensions ($n = 64$): length 537 ± 96 μm (range 350–736 μm), width 396 ± 107 μm (range 224–595 μm), and length/width ratio 1.40 ± 0.24 (range 1.00–2.00). The dimensions of the holotype and four paratypes (Fig. 7A) are given in Table 2. There is quite a wide range in the shape as well as the size of the test. The holotype and seven paratypes were selected as representatives of different shapes and sizes of the test and variations in the apertural structure (Fig. 7A).

There is a single relatively large circular aperture with a slightly produced collar that sometimes comprises several concentric rings (Fig. 8A, B, F–H). The collar is 164–191 μm in diameter ($n = 6$) and 27–40 μm thick ($n = 5$).

The test is flexible, dents readily, especially with handling or when placed in alcohol or RNA*later*™ (Fig. 7B), and is covered with a dense coating of pale mineral grains (Fig. 8C). In reflected light, the test surface is cream or white with a speckled reflective sheen (Figs. 7B, 8A). The test wall is opaque in fresh specimens, obscuring the interior in transmitted light. In formalin, however, sections of the agglutination slough off to reveal a transparent organic wall, 18–25 μm thick ($n = 3$), and the cell body, the interior of which is especially clear when specimens are immersed in glycerol (Fig. 8D, E). The cytoplasm is colourless in live individuals but turns lemon yellow in formalin and RNA*later*™. There is a single nucleus, 72–85 μm in diameter ($n = 3$), typically located at the abapertural end of the cell (Fig. 8D, E). The cytoplasm may also contain partly digested filamentous cyanobacteria (Fig. 8F), diatom frustules (Fig. 8G), and other unidentified ingested items (Fig. 8H) distributed throughout the cell. There are no obvious mineral grains present, and the specimens are not magnetic. A peduncular sheath appears to be present in one specimen (Fig. 8B, G), but this feature is not obvious in other specimens because the view is obscured by agglutinated particles or by the apertural collar (Fig. 8E).

In sediment that has settled in Petri dishes, specimens are visible on the surface, with the abapertural end uppermost and the apertural end buried in the sediment. Since the specimens are brilliant white and relatively large, they are easily seen and can be removed manually with brushes or a pipette and placed on a glass surface. Healthy specimens collect a mass of sediment around the apertural end, which needs to be removed gently to visualise the aperture structures and to observe the profuse set of granulo-reticulopodia that issue from the aperture and are visible under a high-power microscope with phase contrast optics.

Molecular characteristics. *Hilla brevis* (72% BV) forms a strongly supported group (100% BV) with *H. argentea* (Holzmann et al., 2022) and *H. arctica* (Holzmann et al., 2025b) (Table 3; Fig. 3). The partial SSU rDNA sequences of *H. brevis* contain 922 nucleotides, and the GC content is 46–47%. Pairwise sequence distance mounts from 0.002 to 0.07.

Remarks. The type species of the genus, *H. argentea* from South Georgia (Figs. 5 and 6 in Holzmann et al., 2022), has a silvery surface, similar to that of *H. brevis*, but it is much smoother and almost free of any extraneous material. The apertural end is produced into a short tube, rather different from the low collar-like feature of the new species. However, the most striking difference is that *H. argentea* has a very elongate, cylindrical test with a length/width ratio of 5.64–7.53 compared to only 1.0–2.0 in the case of *H. brevis*. In the other described species, *H. arctica* (Fig. 4 in Holzmann et al., 2025b), the test has an intermediate shape and a L/W ratio of 2.6–6.6, bridging the gulf between these two extremes. The apertural structure in *H. arctica* is more similar to that of the type species than to our new species. Another member of Clade Y, undetermined monothalamid 20321 from Greenland (Fig. 12K in Gooday et al., 2022), has a rather similar silvery surface but is also very smooth as well as more elongate than *H. brevis*.

Other silvery saccamminids that resemble the new species include unidentified morphotypes from West Spitsbergen fjords, Svalbard (Fig. 3.8 and particularly Fig. 3.2 in Majewski et al., 2005), and the eastern Clarion Clipperton Zone (CCZ) in the equatorial Pacific (isolate 18549, Fig. A1f in Himmighofen et al., 2023). These are generally smaller than our new species with a smoother surface, and the CCZ specimen is a member of Clade C rather than Clade Y. The Svalbard specimen shown in Figure 3.8 of Majewski et al. (2005) is also spherical, while the CCZ specimen is more elongate and has a more obvious aperture structure. *Senguptiella vestnesensis* from the Vestnesa and Svyatogor Ridge, Arctic Ocean (Figs. 5, 6, 7F, I–L in Holzmann et al., 2025b) is another oval species of similar size but with a smoother silvery test and a more pointed apertural end.

Finally, *H. brevis* resembles *Ovammina opaca* Dahlgren, 1962, also found in our study area, in shape and colour, but has a more flexible and reflective test and an aperture structure with a more pronounced collar. *Hilla brevis* was not encountered in the 2021–2022 collections (Henderson, 2023), but during 2023–2024 it was seen in large numbers throughout the months of sampling, while at the same time the distribution of *O. opaca* was restricted in time and place.

3.1.6. *Flaviatella zaninettiae sp. nov. (Monothalamid Clade Y) (Figs. 9 and 10)*

2023 Saccamminid sp. 3 – Henderson, J. Mar. Biol. Assoc. U.K. 103, e18: 11–12, Fig. 7

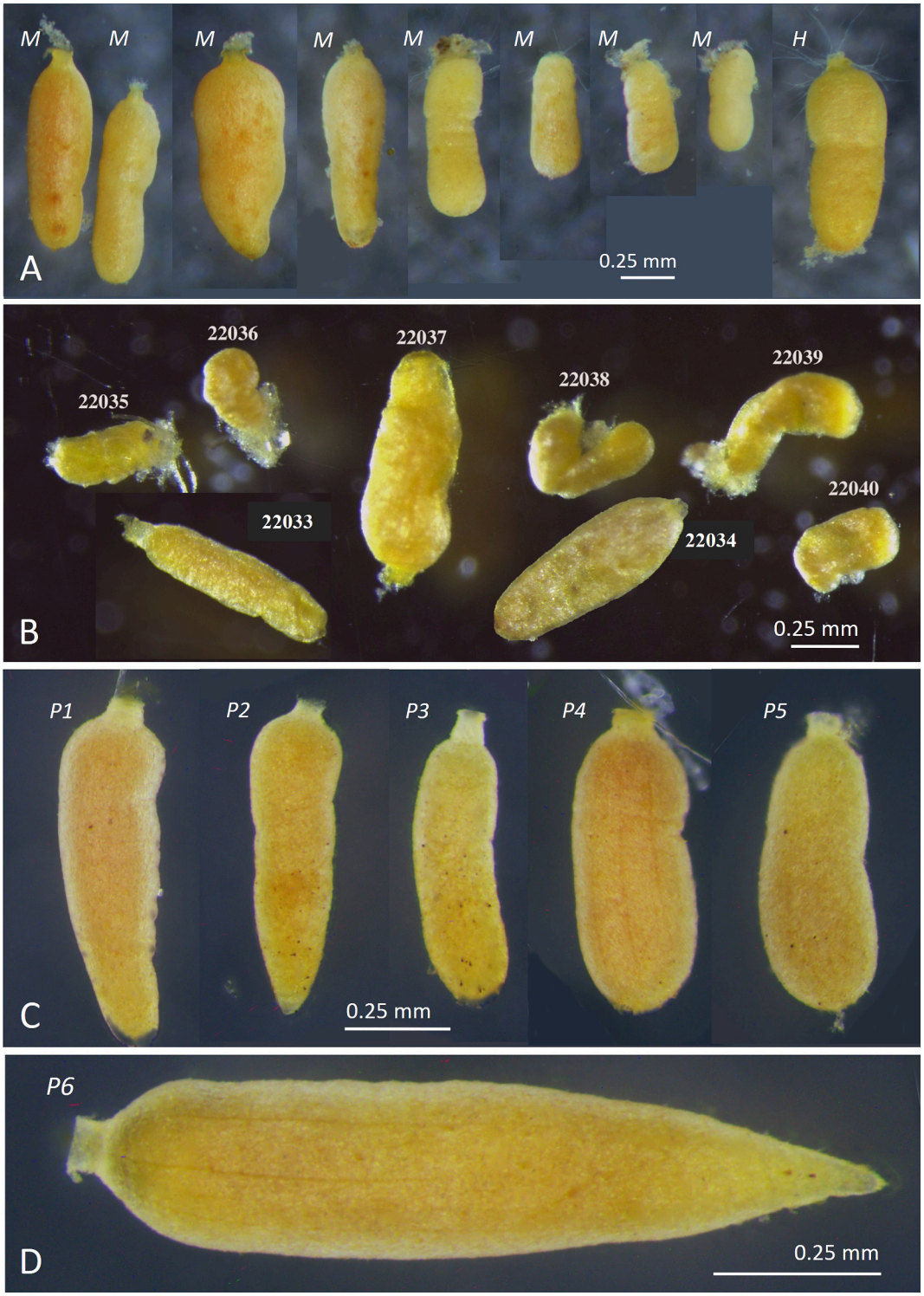

Fig. 9. *Flaviatella zaninettiae* sp. nov. (**A**) Fresh specimens (*M* = destined for molecular analysis; *H* = holotype). (**B**) The specimens labelled "M" now in RNA*later*™; their numbers correspond to subsequently extracted isolates. (**C, D**) Paratypes P1–6 in 10% formalin; fine longitudinal lineations are evident on the surfaces of P4 and P6.

Diagnosis. Test elongate, with a pointed or rounded abapertural end and a short, tubular terminal apertural structure, length 472–1095 µm, width 191–465 µm, length/width ratio 1.93–3.42. Wall 4–10 µm thick, translucent with finely agglutinated veneer and reflective sheen. Cytoplasm visible through the test wall, yellow or orange-coloured in live specimens, but otherwise relatively featureless. No peduncle evident.

Etymology. Named in honor of Louisette Zaninetti, a distinguished micropaleontologist specialized in both fossil and recent foraminifera, who has strongly supported the early research on molecular systematics of this group.

Zoobank registration. The new species-group name *Flaviatella zaninettiae* was registered in ZooBank under the following code: urn:lsid:zoobank.org:act:312DDC76-1D65-43FC-ACB8-DC9E8702CBBB.

Type material (Tables 1 and 2). The type specimens are preserved

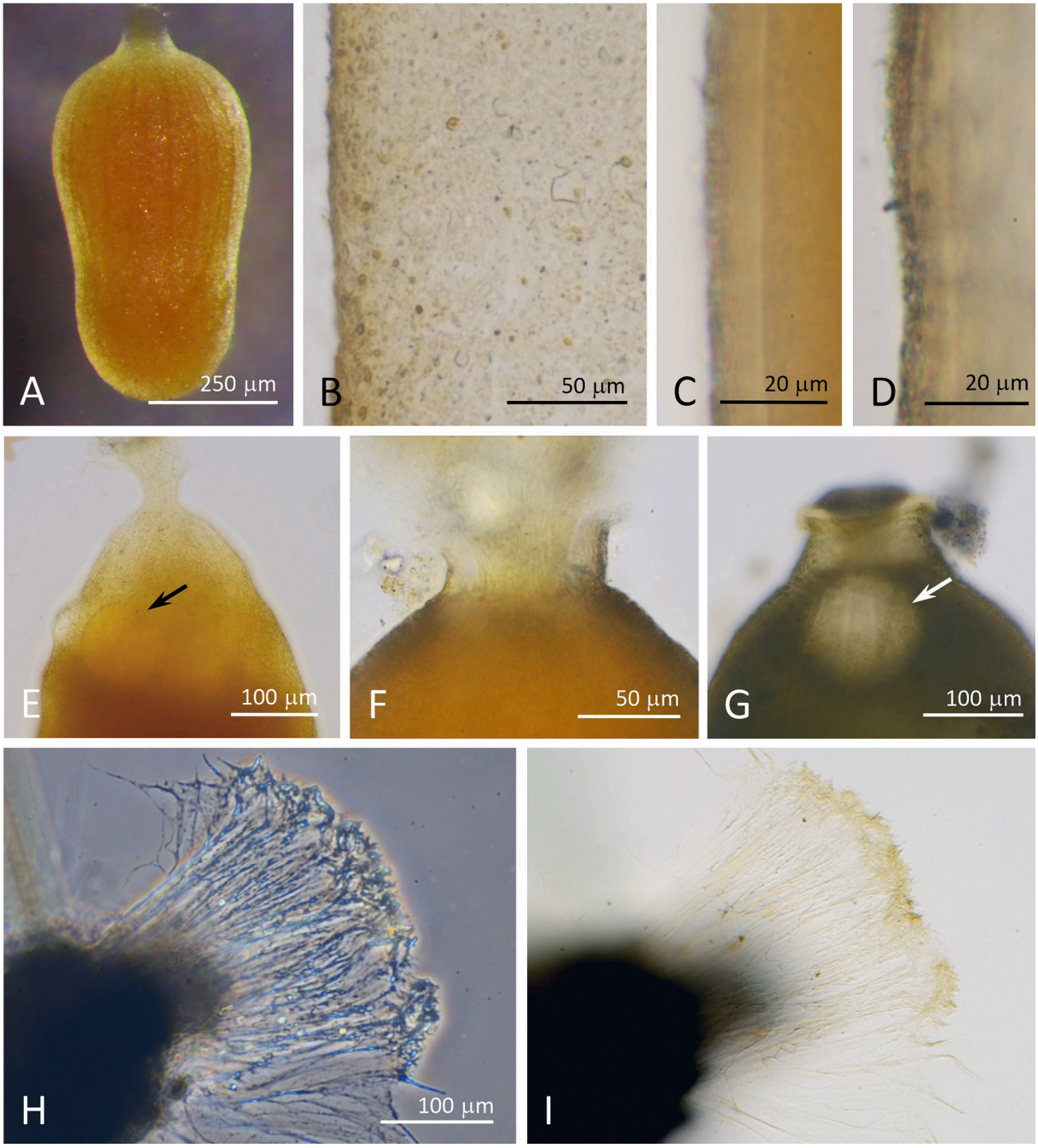

Fig. 10. *Flaviatella zaninettiae* sp. nov., formalin-fixed specimens embedded in glycerol. (**A**) Specimen exhibiting longitudinal lineations on the surface of the test. (**B**) Surface view of the wall of a "ghost" test that had split and lost its contents. (**C, D**) Optical sections of the wall of an intact test and a "ghost" test, respectively. (**E**) Nucleus (arrowed) in naked cytoplasm of a specimen that had lost its test. (**F**) Aperture structure. (**G**) Fresh specimen with nucleus (arrowed). (**H, I**) Granuloreticulopodia containing yellow pigment, as visualised in phase contrast and bright field optics, respectively. (For interpretation of the references to colour in this figure legend, the reader is referred to the web version of this article.)

individually in 10% formalin in 1.5 ml conical screw-cap microcentrifuge tubes (Fisher Scientific) and are deposited in the Natural History Museum, London, under the following registration numbers: Holotype (NHMUK PM ZF 10605) preserved first in isopropyl alcohol and then in 10% formalin, Paratypes 1–6 (NHMUK PM ZF 10606–10611).

Other material (Table 1). Eight specimens for molecular characterisation (isolates 22033–22040) were collected from Site 3. Sequences of another six specimens had been obtained previously and published as undetermined monothalamids (Gooday et al., 2022: isolates 20348, 20350 from Nuuk Fjord, Greenland, Fig. 12M; Holzmann et al., 2025b: isolates 21699–21702 from Vestnesa Ridge, NW Svalbard, Fig. 7G). Twenty-six specimens were collected for morphological analysis from Sites 2 and 3. Included are a description and measurement of one specimen collected in 2021 and which featured in Henderson (2023).

Description based on all material from 2020–2021 and 2023–2024. The test is free, monothalamous and elongate with a simple terminal aperture (Fig. 9) and with the following dimensions ($n = 41$): length 756 ± 159 µm (range 472–1095 µm), width 286 ± 66 µm (range 191–465 µm), and length/width ratio 2.67 ± 0.38 (range 1.93–3.42). The individual dimensions for the holotype and six paratypes are given in Table 2. Although the general shape of the test is cylindrical, the

width often varies within an individual. There is a common tendency for the test to taper towards the abapertural end, in extreme cases tapering to a blunt point so that the test resembles a carrot (Paratypes P1, P2, and P6; Fig. 9C, D). Other relatively wider, more cylindrical specimens have a rounded abapertural end and resemble a marrow (the Holotype in Fig. 9A and Paratypes P3 and P4 in Fig. 9C). Less commonly, the test is somewhat wider at the abapertural end (Paratype P5; Fig. 9C). Specimens that are broader at the apertural end have a curved shoulder to either side of the apertural structure (Fig. 9C). The apertural structure comprises a tubular neck, slightly flared at its end with a simple opening that is sometimes circled by a thin collar (Figs. 9C, D, 10F, G).

The test wall is extremely pliable and sometimes appears wrinkled in live specimens as well as those preserved in alcohol or RNA*later*™ solutions (Fig. 9A, B), although not in formalin (Fig. 9C, D). In reflected light the surface has a metallic sheen and very fine longitudinal lineations are often visible, extending two thirds of the way down from the apertural end (Paratype P4 in Fig. 9C, Paratype P6 in Fig. 9D, and the individual in Fig. 10A). The test is coated with a veneer of fine mineral grains, clearly visible in transmitted light in an empty "ghost" test that had split and lost its cellular contents (Fig. 10B). In optical sections of formalin-fixed specimens immersed in glycerol, the thin test wall appears to have a two-layered structure (Fig. 10C), which is also evident in the "ghost" test wall (Fig. 10D). The thickness of the outer layer is 3–11 μm, and that of the inner layer is < 8 μm, the total thickness being 9–12 μm ($n = 7$). In formalin-fixed specimens immersed in glycerol, granular material becomes discernible in the cytoplasm, most clearly in the "naked" cytoplasm that originated from the "ghost" test (Fig. 10E). However, there are no obvious food items or mineral grains and no discernible peduncle. A single nucleus is present at the apertural end with a diameter of 75–97 μm in fresh material ($n = 3$; Fig. 10G) and 63–81 μm in formalin-fixed specimens embedded in glycerol ($n = 9$; Fig. 10E).

In sediment settled in Petri dishes, the species emerge, or partly emerge, onto the surface with the abapertural end uppermost and the apertural end half-buried in the sediment. The large size, elongate shape, and vivid yellow colour of the specimens render them clearly visible under a stereo-microscope and readily removed with brushes or a pipette and placed on a glass surface. Viable cells collect sediment and detritus around the apertural end, which needs to be removed gently to reveal the tubular aperture structure and to observe the profuse granuloreticulopodia that emanate from it. Observation of the pseudopodia using transmitted light and high-power optics establishes without doubt that the yellow colour of the specimens is due to pigment in the cytoplasm (Fig. 10H, I), which is visible through the test wall and thus imparts the distinct yellow colour of the living specimens.

Comparisons between 2020–2021 and 2023–2024 material from Scotland, and that from Greenland. The largest specimen collected in Scotland during the 2023–2024 period was 1016 μm long and 465 μm wide, comparable in size to the single specimen collected in 2021 (length 1095 μm and width 442 μm; Henderson, 2023). In both cases, the species was found at the lower end of the beach at low tide, close to the river mouth, and in extremely sticky mud, so they could well extend into the sublittoral zone. They were most abundant in the autumn of 2023 and apparently confined to the shores of Loch Creran. Specimens now determined to be of the same species from the Nuuk Fjord, Greenland ($n = 2$) measured 1166 μm and 1500 μm in length and 83 μm to 167 μm in width, and those from the Vestnesa Ridge, NW Svalbard ($n = 4$) measured 1016 μm to 1563 μm in length and 208 μm to 365 μm in width; the mean length/width ratio for the latter six is 7.0, compared to 2.67 ($n = 41$) for the Scottish specimens.

Molecular characteristics. *Flaviatella zaninettiae* (86% BV) forms a group with *F. siemensma* and *F. profunda* (Holzmann et al., 2025a). The branching is supported by 77% BV (Table 3; Fig. 3). The partial SSU rDNA sequences of *F. zaninettiae* contain 795 nucleotides (isolates 20348, 20350, 21699–21702) and 906 nucleotides (isolates 22033–22040). The difference in sequence length is due to different primers used for amplification; reverse primer sB was used for the present study, while reverse primer s20 was used in previous studies (Gooday et al., 2022; Holzmann et al., 2024). The GC content is 47–48%. Pairwise sequence distance mounts from 0 to 0.003.

Remarks. Molecular data confirm that *F. zaninettiae* is also present in samples from Nuuk Fjord, Greenland, and from Vestnesa Ridge, NW Svalbard, located at 79° N and > 1200 m depth. The sequences of the individuals from Greenland, Vestnesa Ridge, and Scotland are almost identical and differ only in three nucleotide positions. The Scottish *F. zaninettiae* specimens are from nearshore samples, whereas the ones from Greenland were sampled at 61 m depth and from Vestnesa Ridge at 1397 m depth (Gooday et al., 2022; Holzmann et al., 2025b). This is an unusually wide distribution, as the species seems to occur in both temperate and Arctic environments and from coastal to upper bathyal. Certain foraminiferal morphospecies have wide or very wide bathymetric ranges. These include the multichambered *Adercotryma glomeratum* (Brady, 1878), reported from coastal to hadal depths, although this has not been characterised molecularly and may be a composite of several cryptic species. The genetically characterised species with a very wide bathymetric range include *Bathyallogromia weddellensis*, sampled at 1000 to 6000 m in the Weddell Sea (Gooday et al., 2004), and *Epistominella vitrea* Parker, 1953, now known as *Eilohedra vitrea* (Parker, 1953), found from sublittoral to bathyal depths in the Antarctic (~60 to > 1000 m; Pawlowski et al., 2007). These ranges are not unexpected, as there is a tendency for species to have wider depth distributions in the Arctic and Antarctic ('polar emergence') because the water column is more isothermal.

Flaviatella zaninettiae closely resembles *F. siemensma* from the Falkland Islands (Holzmann et al., 2025a). A *Nemogullmia*-like monothalamid (isolate 19859) from the Nuuk Fjord, Greenland (Fig. 12L in Gooday et al., 2022), which is also a member of Clade Y and has similarly distinctive yellow cytoplasm, is much more elongated than *F. zaninettiae*. *Nujappikia idaliae*, another member of Clade Y from the Nuuk Fjord (Figs. 4–7 in Gooday et al., 2022), has white rather than yellow cytoplasm and a more evenly cylindrical test.

Flaviatella zaninettiae is somewhat similar in shape to *Phainogullmia aurata* Nyholm, 1955 from the Gullmar Fjord (Nyholm, 1955), and illustrated by Loeblich and Tappan (1987, Plate 8, Figs. 5, 6), who described it as having a cylindrical test 0.2–1.4 mm in length with a glossy yellowish-brown, flexible test wall. Majewski et al. (2005, Fig. 3.7 therein) illustrated a carrot-shaped specimen of *Phainogullmia* sp. rather similar in shape to ours, shown in Figure 9D. However, the wall of *Phainogullmia* sp. is opaque rather than translucent, has a reflective surface, and bears apertures at each end of the test. Species of *Gloiogullmia* Nyholm, 1974 (e.g., Figs. 2.10, 11 in Majewski et al., 2007; Fig. 2A–C in Pawlowski et al., 2008) are also rather similar in general shape, but have a purely organic test devoid of agglutinated particles and group within monothalamid Clade C (Holzmann et al., 2022). *Flaviatella zaninettiae* differs from *Limaxia alba*, a species that groups in monothalamid Clade A, in having a more variable test morphology, a test wall with an agglutinated veneer rather than being largely organic, and a yellow rather than white cytoplasm (Figs. 7 and 10 in Holzmann et al., 2022).

3.1.7. Flexammina islandica Voltski & Pawlowski, 2015 (Monothalamid Clade M) (Fig. 11)

2015 *Flexammina islandica* Voltski & Pawlowski, Zootaxa 3964: 247–250, Plate 1, Figs. A–I

2023 Agglutinated dome 1 – Henderson, J. Mar. Biol. Assoc. U.K. 103, e18: 14–16, Figs. 11 and 12

Diagnosis (modified from Voltski and Pawlowski, 2015). Test free or attached, monothalamous, subspherical or elongated when free, but showing significant shape plasticity when attached. Test diameter 133–835 μm, length/width ratio 1.00–2.91. Aperture subcircular to irregular, surrounded by a short collar. Test wall flexible and opaque; surface white, matt, non-reflective, formed by a thick layer of mineral

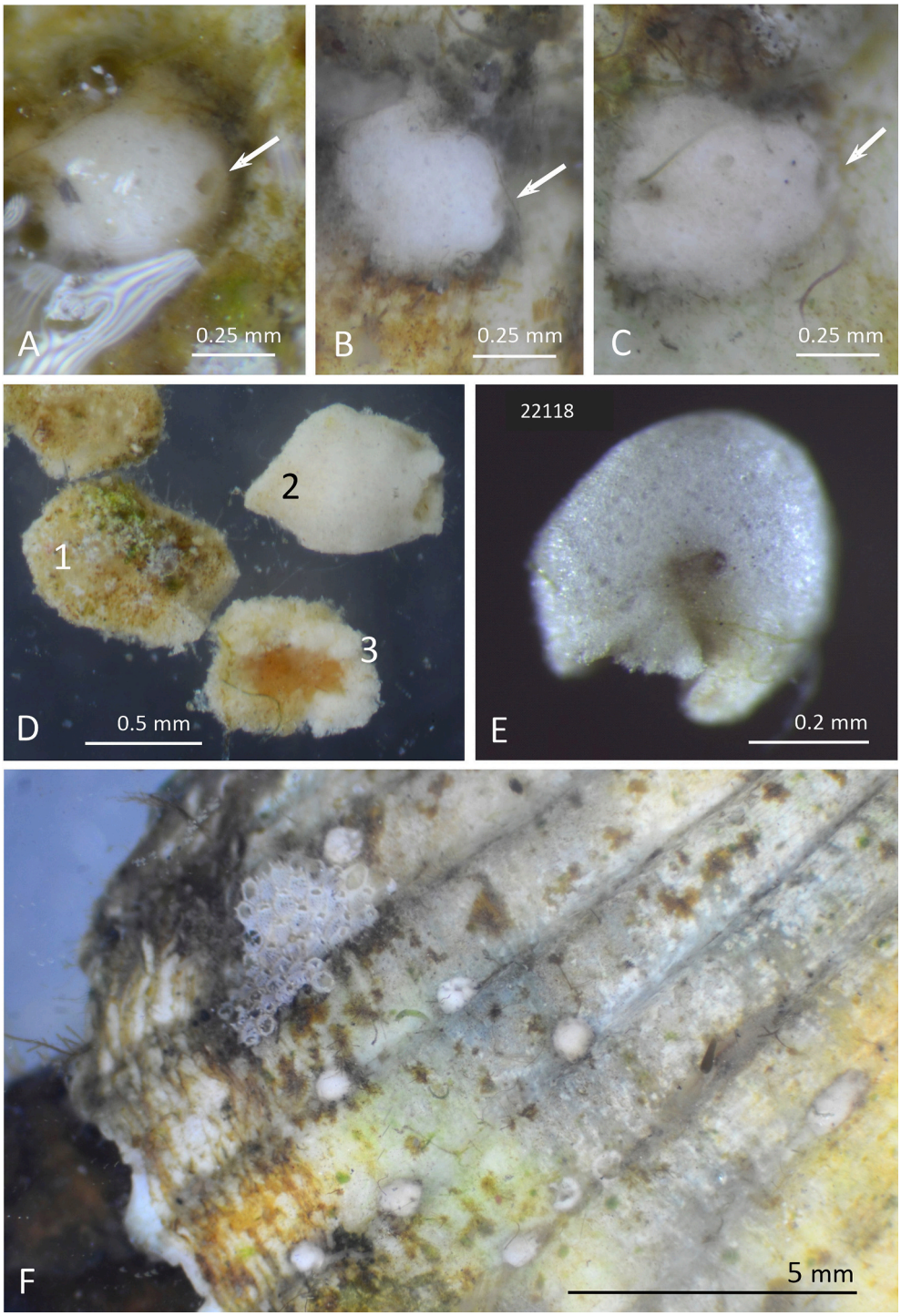

Fig. 11. *Flexammina islandica* Voltski & Pawlowski, 2015. (**A–C**) Live specimens attached to a bivalve shell; apertures are indicated by arrows. (**D**) Three specimens after removal from their substrates: No.1 with intact basal-attachment of its test, No. 2 showing the top view of its test, and No. 3 lacking the basal-attachment of its test to reveal an orange-coloured cytoplasm within. (**E**) Specimen destined for molecular determination in RNA*later*™; its number corresponds to the subsequently extracted isolate. (**F**) A cluster of attached specimens on a bivalve shell.

grains with an underlying layer of organic material.

Material (Table 1). One specimen for molecular characterisation (isolate 22118) and six specimens for morphological analysis were collected from Site 2. Another specimen for molecular characterisation (isolate 22119) and three specimens for morphological analysis were collected from Site 4. Also included are descriptions and measurements of 47 specimens collected in 2020–2021 and reported in Henderson (2023).

Description based on all material from 2020–2021 and 2023. The test is dome-shaped with an irregular outline (Fig. 11) and has the following dimensions (n = 58): length 511 ± 197 μm (range 133–835 μm), width 399 ± 169 μm (range 120–712 μm), and length/width ratio 1.32 ± 0.30 (range 1.00–2.91). A circular or oval aperture, bounded by an agglutinated collar, is located eccentrically, usually close to the rim of the test (Fig. 11A–C). The test wall is opaque and the surface is white and non-reflective, consisting of a layer of fine agglutinated mineral particles

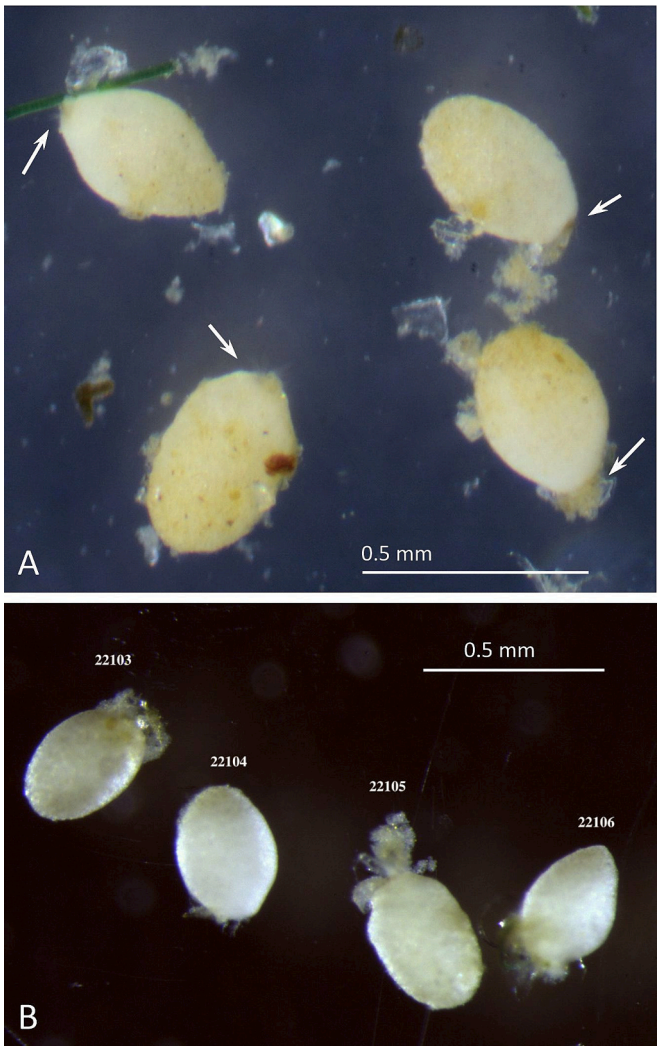

Fig. 12. *Ovammina opaca* Dahlgren, 1962. (**A**) Live specimens destined for molecular characterisation (apertures are arrowed). (**B**) The same specimens now in RNA*later*™; their numbers correspond to subsequently extracted isolates.

(Fig. 11A–E).

Specimens settle on hard substrate but do not seem to prefer a particular type. They are found attached, for example, to pieces of the smaller species of red seaweeds, pebbles, or empty shells of molluscs and usually occur in groups (Fig. 11F). Those living on seaweed are often attached at inner branching points and conform to the contours of the branches. However, most apparently suitable substrates are not utilised. Living specimens are firmly attached to the substrate and covered with sediment, which can be gently brushed away with a fine artist's brush to reveal the underlying dome. They may be released from the substrate by a gentle sideways nudge with fine forceps, an action that often causes the dome of the test to detach from the thinner basal part of the test that remains adhered firmly to its substrate (Fig. 11D). Turning the detached specimens over reveals colourless or orange cytoplasm that fills the entire test cavity (Fig. 11D) and which remains viable and capable of producing a rich array of granulo-reticulopodia visible under high-power phase contrast. The thickness of the test wall, measured approximately across broken edges of released specimens, is in the range 10–50 μm ($n = 8$).

Comparison between 2020–2021 and 2023 material. Specimens collected in 2020–2021 (Henderson, 2023) had the following dimensions ($n = 47$): length 475 ± 197 μm (range 133–833 μm), width 362 ± 163 μm (range 120–712 μm), and length/width ratio 1.35 ± 0.33 (range 1.00–2.91). Those collected in 2023 ($n = 11$) were significantly larger ($p < 0.05$, *t*-test): length 666 ± 103 μm (range 528–835 μm), width 559 ± 80 μm (range 433–685 μm), and length/width ratio 1.19 ± 0.10 (range 1.04–1.38). The size difference may reflect a bias towards collecting larger specimens for molecular characterisation, since smaller individuals are liable to be damaged when being dislodged from the substrate.

Remarks. The identity of this species is confirmed by the genetic data (Table 3; Fig. 3). In terms of morphology, the Scottish specimens conform well to the description and illustrations of the original Icelandic specimens (Voltski and Pawlowski, 2015), except that these occurred as free as well as attached tests, whereas all of the Scottish specimens were attached. Like the attached forms, the free specimens described by Voltski and Pawlowski (2015) are domed and cannot be confused easily with other free-living white saccamminids.

A number of sessile monothalamids resemble *F. islandica*, among them *Crithionina mamilla* Goës, 1894, *Hemisphaerammina batalleri* Loeblich & Tappan, 1957, *Pseudowebbinella goesi* (Höglund, 1947), *Tholosina protea* Heron-Allen & Earland, 1932. As discussed by Voltski and Pawlowski (2015), the first three species are clearly different. In *Crithionina mamilla*, there is no aperture; the test wall is spongy and very thick in relation to the cavity; and the agglutination comprises large and small particles (Goës, 1894; Höglund, 1947). In *Hemisphaerammina batalleri*, there is no basal rim, no aperture, the test wall is again thick in relation to the cavity and includes both large and small mineral particles (Loeblich and Tappan, 1987), and most crucially, molecular data assigns it to Clade F rather than Clade M (Voltski and Pawlowski, 2015). *Pseudowebbinella goesi* is more similar to *F. islandica* in being free or detached, with a finely agglutinated test wall and a smooth white surface. However, its test is larger (1–3 mm diameter), apparently lacks an aperture, and the cavity is incompletely subdivided by irregular partitions (Höglund, 1947). *Tholosina protea* Heron-Allen & Earland, 1932 is dome-shaped on flat surfaces but can also adopt the contours of its substrate, thereby taking on an irregular shape, for example, sitting in a fork or wrapping around the branch of a "zoophyte" (Heron-Allen and Earland, 1932). It is composed of fine mineral grains with a "smooth but not polished" surface, and its apertures apparently comprise one or more small holes situated at the extremities. Although described from the South Atlantic, the species has also been reported from British waters (Rhumbler, 1935). The morphological description is reminiscent of *F. islandica*, but the relationship between these species cannot be clarified in the absence of molecular data for *T. protea*.

3.1.8. Ovammina opaca Dahlgren, 1962 (Monothalamid Clade O) (Fig. 12)

1962 *Ovammina opaca* Dahlgren, Zool. Bidr. Uppsala 33: 197–199, Fig. 1, Plate 1

1987 *Ovammina opaca* Dahlgren, 1962 – Loeblich and Tappan, Foraminiferal Genera and their Classification, p. 31, Plate 22, Fig. 10

2011 *Ovammina opaca* Dahlgren – Goldstein and Alve, Mar. Ecol. Prog. Ser. 437: 4, Fig. 3f

2023 Saccamminid sp. 1 – Henderson, J. Mar. Biol. Assoc. U.K. 103, e18: 9–11, Fig. 5

Diagnosis (modified from Loeblich and Tappan, 1987). Test free, monothalamous, ovoid to fusiform, length 130–700 μm, width 130–500 μm, ovoid to circular in transverse section. Wall with an inner hyaline layer and an outer opaque layer of fine agglutinated mica flakes and diatom frustules, creating a granular surface. Aperture terminal, with a peduncular sheath (entosolenian apparatus) having a diameter about one-fourth to one-sixth of the test diameter, connected to the inner wall layer by thin lateral lamellae. During gametogenesis the main aperture constricts and closes, and a ring of accessory apertures forms around it to provide egress for the gametes.

Material (Table 1). Four specimens for molecular characterisation (isolates 22103–22106) were collected from Site 1, and three specimens

for morphological analysis from Site 2. Also included are descriptions and measurements of 43 specimens collected in 2020–2021 and reported in Henderson (2023).

Description based on all material from 2020–2021 and 2023. The test is broadly oval, widest near the midpoint and with a rounded or slightly pointed abapertural end (Fig. 12). Dimensions are (n = 50): length 341 ± 58 μm (range 188–448 μm), width 240 ± 46 μm (range 131–333 μm), and length/width ratio 1.43 ± 0.13 (range 1.13–1.75). There is a single terminal aperture structure, either a simple featureless opening or an opening surrounded by a collar (Fig. 12). The test wall is opaque and the internal contents are not visible, even in specimens embedded in glycerol. The specimens are not magnetic. The surface of the test is cream or white, grading to yellow or orange towards the abapertural end; the orange colour is more prominent in specimens collected during the autumn months. The test wall is relatively rigid compared to other whitish saccamminid species, although it may distort when preserved in alcohol.

When sediment is settled in Petri dishes, the species emerges onto the surface, with the abapertural end uppermost and the apertural end buried in the sediment. Specimens removed manually display a rich deposit of sediment around the apertural end and profuse granulopseudopodia, which are visible under high-power phase contrast.

Comparison between 2020–2021 and 2023 material. The 2020–2021 specimens of *O. opaca* from Scotland had the following dimensions (n = 43): length 335 ± 59 μm (range 188–448 μm), width 235 ± 48 μm (range 131–333 μm), and length/width ratio 1.44 ± 0.13 (range 1.13–1.75). The dimensions of those from 2023 (n = 7) were: length 378 ± 36 μm (range 313–421 μm), width 266 ± 12 μm (range 243–278 μm), and length/width ratio 1.42 ± 0.09 (range 1.29–1.56). The second cohort had a more restricted width range, but this probably reflected the much smaller sample size. However, there were no significant differences in the dimensions of the two groups.

Remarks. Our specimens are very similar in general appearance to *O. opaca* as described by Dahlgren (1962) from 1 m depth on a "detritus-covered muddy sand bottom" in the Gullmar Fjord, Swedish west coast. In terms of size, most specimens were comparable to the measurements of length (300–400 μm) and width (half of the length) given by Dahlgren (1962), although he also found some larger individuals (up to 700 μm). Our intertidal samples yielded many white saccamminids that resembled *O. opaca* and were difficult to separate morphologically (Henderson, 2023). The identification of this species was therefore dependent on molecular data (Table 3; Fig. 3), which grouped it close to two sequences in Clade O assigned to *O. opaca* (Gooday et al., 2011; Voltski and Pawlowski, 2015). However, it should be noted that these existing sequences were from specimens collected in the Barents Sea (isolate 2485) and from Nissum on the west coast of Denmark (isolate 2399), rather than from the type locality, and were slightly different from our sequences. Identification of the Scottish specimens as *O. opaca* therefore requires confirmation. Undetermined Monothalamid 2 of Henderson (2023; Fig. 8A–D therein) is a small saccamminid similar in appearance to *O. opaca* and could well have been a juvenile form.

In this study, we only examined the external appearance of the test of *O. opaca*. Dahlgren (1962) provides more details about the test structure. He describes a rather complicated "apertural apparatus" (presumably the entosolenian apparatus of Loeblich and Tappan, 1987), with the opening being surrounded by a collar and extending inwards into a "cylindrical apertural sheath" that enlarges into an "inner, flattened apertural sheath" with a lenticular cross-section. The lateral angles of this inner sheath are connected by a "thin lamella" to the inner layer of the wall. The test wall itself is relatively robust, with an inner organic layer overlain by a much thicker, finely agglutinated outer layer, the combined thickness being about 17 μm. The thick wall may provide the test with a degree of rigidity that is unusual for soft-walled saccamminids. During the sexual reproductive stage of the life cycle, the test develops a ring of holes in the test wall around the aperture for the release of bi-flagellated gametes (Dahlgren, 1962, 1964; Goldstein and Barker, 1990; Korsun et al., 2014). Ten such specimens, which appeared to be dead, were also found at the Scottish sites in 2021, and these were significantly larger on average than the live specimens (Henderson, 2023).

Ovammina opaca is very similar morphologically to *O. patagoniensis* (Lena, 1974) from Puerto Deseado, Argentina. Lena (1974) assigned her species to a new genus, *Dahlgrenia*, based on the structure of the nuclei, but in most other respects it appears identical to *O. opaca*, and indeed *Dahlgrenia* has since been synonymised with the genus *Ovammina* by the World Register of Marine Species. The main differences appear to be the smaller size of the test (length 130–220 μm) and the even thicker wall (19.0–38.5 μm) of *O. patagoniensis*. Another member of Clade O, *Cedhagenia saltatus*, described from the coast of the Crimea Peninsula in the Black Sea, has a rather lenticular shape with a more or less bluntly pointed abapertural end, an aperture located at the end of a short tubular extension, and a thinner, more flexible wall (Gooday et al., 2011).

Ovammina opaca was widespread in firm and sticky sediment at several sites in the Lorne area in 2020 and 2021 (Henderson, 2023), and at two sites in the autumn of 2023, but was not found in 2024. In addition to the west coast of Scotland, the Gullmar Fjord, Sweden (Dahlgren, 1962), the west coast of Denmark, and the Barents Sea, it has been reported from Sapelo Island, Georgia, U.S.A (Goldstein and Alve, 2011), and some rather doubtful specimens from the Arabian Sea (Ranju et al., 2017).

3.2. Molecular phylogeny

The obtained sequences cluster in five different monothalamid clades (Fig. 3). *Flexammina islandica* (Clade M) branches with specimens described from Iceland (100% BV) and clusters as sister to Clade E; the branching of these two clades is highly supported (91% BV). *Psammophaga owensi* (88% BV) is a member of Clade E and branches as sister to *Psammophaga* spp. obtained from Oban Bay and Aarhus Bay (Table 3; Fig. 3), with their branching supported by 83% BV. *Psammophaga zirconia*, *P. fuegia* (Gschwend et al., 2016), *P. secriensia*, and *P. magnetica* are the closest relatives of *P. owensi* and *Psammophaga* sp. Clade E is moderately supported (71% BV). The branching of Clade O (*O. opaca*, *C. saltatus*) and Clade Y is supported by 74% BV. Both clades themselves are highly supported (99% and 100% BV, respectively). Clade Y contains seven taxa. Within this clade, the branching of *H. arctica*, *H. argentea*, and *H. brevis* is highly supported (100% BV). *Nujappikia idaliae* clusters at the base of *Flaviatella* spp., but this branching is not supported by BV. Clade D (100% BV) clusters at the base of the aforementioned clades. *Lorneia ovalis* (100% BV) and *L. sphaerica* (97% BV) branch at the base of *Hippocrepinella* spp.

4. Discussion

Based on a combination of morphological and molecular data, we describe five new monothalamid species, together with two that were already established, from small estuarine bays in northwest Scotland, located mainly at the mouths of fjord-like lochs and fed by a combination of freshwater and seawater. With one exception, *Toxisarcon alba* of Wilding (2002), this is the first time that soft-walled monothalamids have been formally described from this kind of environment. There are a few previous records of monothalamids from estuaries, but unlike our study sites, they are all associated with large rivers feeding directly into the sea (e.g., Ellison, 1984; Gooday and Fernando, 1992; Singer et al., 2023). Most other coastal monothalamid species described during the past few decades have originated from mudflats or salt marshes (e.g., Altin et al., 2009; Altin-Ballero et al., 2013; Goldstein and Barker, 1988; Goldstein et al., 2010) or from freshwater habitats (Siemensma and Holzmann, 2023; Siemensma et al., 2017, 2021). Compared to these relatively meagre observations, there is a growing body of literature on monothalamids from the bathyal, abyssal, and hadal deep sea and high

latitude settings (e.g., Cedhagen et al., 2009; Gooday et al., 2020, 2021, 2022; Holzmann et al., 2022, 2025a; Pawlowski and Majewski, 2011; Pawlowski et al., 2025; Sabbatini et al., 2004; Sinniger et al., 2008). An important aspect of the present study, therefore, is the support it gives to previous evidence (e.g., Habura et al., 2008; Singer et al., 2023) that monothalamids are locally as important and diverse in easily accessible, temperate, shallow-water habitats as they are in these more remote locations. Where they have been the target of a focused research effort, as around the Crimean Peninsula and other parts of the Black Sea and adjacent waters (reviewed by Sergeeva and Anikeeva, 2024), monothalamids have proved to be a diverse and abundant component of the benthic coastal meiofauna.

At larger regional scales, the spatially heterogeneous nature of coastal environments is likely to enhance foraminiferal diversity. Different assemblages can be found in habitats as varied as rocky shores, deltas, bays, lagoons, fjords, mudflats, and salt marshes (e.g., Murray, 2006; Phleger, 1960), their composition being influenced by multiple factors, among which salinity and sediment characteristics may be particularly important in estuaries (Fouet et al., 2022). As a result, foraminiferal species often have narrower geographical ranges in coastal and sublittoral settings than in the deep sea and particularly on abyssal plains (Culver and Buzas, 1998; Gooday and Jorissen, 2012; Hayward and Holzmann, 2023). Assemblage composition in estuaries and salt marshes can display seasonal as well as spatial patterns, particularly in response to fluctuations in food supply (e.g., algal blooms: Debenay et al., 2006; Lee et al., 1969; Murray, 1983). This may serve to further enhance monothalamid diversity by facilitating species coexistence. On the other hand, a number of factors probably contribute to the underestimation of monothalamid diversity in estuarine and other coastal settings (Singer et al., 2023). The complexity of near-shore habitats and the fluctuating environmental influences to which monothalamid and other foraminiferal species are subjected makes it more likely that species will be missed during sampling, either because they are represented by dormant propagules or confined to very localised patches of the habitat (Buzas et al., 2002, 2015). There may also be numerous monothalamids that are too small and delicate to extract from sieved mud samples for morphological and genetic analysis. Most importantly, the low fossilisation potential of many species means that they are commonly ignored in studies that have a micro-palaeontological focus. All of these factors may contribute to the underestimation of foraminiferal diversity in shallow and intertidal habitats.

An interesting aspect of the Lorne assemblages is that they include two species, *Hilla brevis* and *Flaviatella zaninettiae*, with genetically related deep-sea counterparts. The type species *Hilla argentea* was described from the littoral zone of the subantarctic island of South Georgia, but a second species, *H. arctica*, is present off the coast of NW Svalbard at about 1200 m depth (Holzmann et al., 2025b). *Flaviatella profunda* was sampled at abyssal depths close to the Japan Trench and Aleutian Trench, and *F. siemensma* in a shallow bay area in East Falkland. *Flaviatella zaninettiae* was also sampled in the Nuuk Fjord system and in the deep water of NW Svalbard. The monothalamid genus *Bathyallogromia* Gooday et al., 2004, not represented in our collections, includes a similar mixture of deep and shallow-water species, the first described from the deep Weddell Sea (*B. weddellensis* Gooday et al., 2004) and two others from Greenland (*B. kalaallita* Gooday et al., 2022) and the fjords of South Georgia (*B. olivacea* Holzmann et al., 2022). These wide distributions are consistent with previous observations of bipolar distributions in monothalamid foraminifera (Pawlowski et al., 2008). Our results provide further examples of monothalamid genera that are distributed over a wide geographical and bathymetric range and are able to adapt to different environmental conditions. The deep-sea representatives of these genera are most common in bathyal continental margin settings. On the other hand, they and the Lorne monothalamids, which typically have simple, mainly rounded or flask-shaped morphologies, have little in common with the delicate, largely undescribed and problematic forms with much more complex morphologies that typically dominate the meiofauna, macrofauna, and even the megafauna of abyssal plains (Goineau and Gooday, 2019; Gooday and Wawrzyniak-Wydrowska, 2023; Gooday et al., 2017).

In conclusion, we have described, based on both morphological and molecular data, a number of species that are a part of the considerable diversity of monothalamid foraminifera populating the Lorne intertidal area of northwest Scotland. These and other coastal monothalamids have simple shapes, comparable to those of some freshwater foraminifera and in contrast to the more heterogeneous deep-sea assemblages. The current study underlines the importance of molecular and morphological characteristics for correctly identifying and describing single-chambered foraminifera. Our description of species in the Lorne area is by no means comprehensive, and it is likely that many species remain undiscovered. Foraminifera living in coastal and particularly intertidal habitats are subject to more variable conditions than those in deeper waters. Only a few active species will dominate the community at any one time, the remainder lying dormant as propagules and potentially ready to form blooms as soon as the conditions become more favourable for them (Alve and Goldstein, 2010; Goldstein and Alve, 2011; Singer et al., 2023). A much more comprehensive and long-term study will be necessary in order to reveal the full extent of monothalamid diversity in this geographically heterogeneous area.

CRediT authorship contribution statement

Zaineb Henderson: Writing – review & editing, Writing – original draft, Visualization, Resources, Investigation, Formal analysis, Data curation, Conceptualization. **Maria Holzmann:** Writing – review & editing, Writing – original draft, Visualization, Validation, Resources, Investigation, Funding acquisition, Formal analysis, Data curation, Conceptualization. **Andrew J. Gooday:** Writing – review & editing, Writing – original draft, Validation, Investigation, Conceptualization.

Funding

Maria Holzmann acknowledges support from the Schmidheiny Foundation, under a grant entitled: 'Exploring abyssal and hadal biodiversity of foraminifera in the North Pacific'.

Acknowledgments

Thanks are to the following members of staff at the Scottish Association for Marine Science (SAMS, https://www.sams.ac.uk/): Professor Nick Owens (Director) and Professor Axel Miller (Deputy Director) for permission to use facilities at SAMS, and Nicola Cook, Christopher Clay, Naomi Thomas and Dr. Gail Twigg for provision of reagents and laboratory space, and for health and safety inductions. Acknowledged also is the University of Leeds for providing Zaineb Henderson (as a Visiting Senior Research Fellow) with access to the university library services.

Data availability

All data generated and analysed during this study are included in this published article. The sequences were submitted to GenBank (https://www.ncbi.nlm.nih.gov) under the following accession numbers: PV072525–PV072554. Specimens of the new species are housed in the collections of the Natural History Museum, London.

References

Altin, D.Z., Habura, A., Goldstein, S.T., 2009. A new allogromiid foraminifer *Niveus flexilis* nov. gen., nov. sp., from coastal Georgia, USA: fine structure and gametogenesis. J. Foramin. Res. 39, 73–86. https://doi.org/10.2113/gsjfr.39.2.73.

Altin-Ballero, D., Habura, A., Goldstein, S., 2013. *Psammophaga sapela* n. sp., a new monothalamous foraminiferan from coastal Georgia, U.S.A.: fine structure, gametogenesis and phylogenetic placement. J. Foramin. Res. 43, 113–126. https://doi.org/10.2113/gsjfr.43.2.113.

Alve, E., Goldstein, S.T., 2010. Dispersal, survival and delayed growth of benthic foraminiferal propagules. J. Sea Res. 63, 36–51. https://doi.org/10.1016/j.seares.2009.09.003.

Barrenechea Angeles, I., Nguyen, N.-L., Greco, M., Tan, K.S., Pawlowski, J., 2024. Assigning the unassigned: a signature-based classification of rDNA metabarcodes reveals new deep-sea diversity. PloS ONE 19, e0298440. https://doi.org/10.1371/journal.pone.0298440.

Brady, H.B., 1878. On the reticularian and radiolarian Rhizopoda (Foraminifera and Polycystina) of the North-Polar Expedition of 1875–76. Annals Mag. Nat. Hist. (Ser. 5) 1 (6), 425–440. https://doi.org/10.1080/00222937808682361.

Burki, F., Roger, A.J., Brown, M.W., Simpson, A.G.B., 2020. The new tree of eukaryotes. Trends Ecol. Evol. 35, 43–55. https://doi.org/10.1016/j.tree.2019.08.008.

Buzas, M.A., Hayek, L.-A.C., Reed, S.A., Jett, J.A., 2002. Foraminiferal densities over five years in the Indian River lagoon, Florida: a model of pulsating patches. J. Foramin. Res. 32, 68–92. doi: 10.2113/0320068.

Buzas, M.A., Hayek, L.-A.C., Jett, J.A., Reed, S.A., 2015. Pulsating Patches: History and Analyses of Spatial, Seasonal, and Yearly Distribution of Living Benthic Foraminifera. Smithsonian Contributions to Paleobiology, Number 97. Smithsonian Institution Scholarly Press, Washington, D.C. https://doi.org/10.5479/si.19436688.97.

Cavalier-Smith, T., 1999. Principles of protein and lipid targeting in secondary symbiogenesis: euglenoid, dinoflagellate, and sporozoan plastid origins and the eukaryote family tree. J. Eukaryot. Microbiol. 46, 347–366. https://doi.org/10.1111/j.1550-7408.1999.tb04614.x.

Cavalier-Smith, T., 2002. The phagotrophic origin of eukaryotes and phylogenetic classification of Protozoa. Int. J. Syst. Evol. Microbiol. 52, 297–354. https://doi.org/10.1099/00207713-52-2-297.

Cedhagen, T., Gooday, A.J., Pawlowski, J., 2009. A new genus and two new species of saccamminid foraminiferans (Protista, Rhizaria) from the deep Southern Ocean. Zootaxa 2096, 9–22. https://doi.org/10.11646/zootaxa.2096.1.3.

Cordier, T., Angeles, I.B., Henry, N., Lejzerowicz, F., Berney, C., Morard, R., Brandt, A., Cambon-Bonavita, M.A., Guidi, L., Lombard, F., Arbizu, P.M., Massana, R., Orejas, C., Poulain, J., Smith, C.R., Wincker, P., Arnaud-Haond, S., Gooday, A.J., de Vargas, C., Pawlowski, J., 2022. Patterns of eukaryotic diversity from the surface to the deep-ocean sediment. Sci. Adv. 8, eabj9309. https://doi.org/10.1126/sciadv.abj9309.

Culver, S.J., Buzas, M.A., 1998. Patterns of occurrence of benthic foraminifera in time and space. In: Donovan, S.K., Paul, C.R.C. (Eds.), The Adequacy of the Fossil Record. Cambridge University Press, New York, NY, pp. 207–226.

Dahlgren, L., 1962. A new monothalamous foraminifer, *Ovammina opaca* n. gen., n. sp., belonging to the family Saccamminidae. Zool. Bidr. Uppsala 33, 197–200.

Dahlgren, L., 1964. On nuclear cytology and reproduction in the monothalamous formanifer *Ovammina opaca* Dahlgren. Zool. Bidr. Uppsala 36, 1–27.

Day, J.W., Kemp, W.M., Yánez-Arancibia, A., Crump, B.C. (Eds.), 2012. Estuarine Ecology, 2nd ed. Wiley-Blackwell, Hoboken, N.J.

Debenay, J.P., Bicchi, E., Goubert, E., Armynot du Châtelet, E., 2006. Spatio-temporal distribution of benthic foraminifera in relation to estuarine dynamics (Vie estuary, Vendée, W France). Estuar. Coast. Shelf Sci. 67, 181–197. https://doi.org/10.1016/j.ecss.2005.11.014.

d'Orbigny, A.D., 1826. Tableau méthodique de la classe des Céphalopodes. Ann. Sci. Nat. 7, 245–314.

Ellison, R.L., 1984. Foraminifera and meiofauna on an intertidal mudflat, Cornwall, England: populations, respiration, secondary production and energy budget. Hydrobiologia 109, 131–148. https://doi.org/10.1007/BF00011572.

Fouet, M.P.A., Singer, D., Coynel, A., Heliot, S., Howa, H., Lalande, J., Mouret, A., Schweizer, M., Tcherkez, G., Jorissen, F.J., 2022. Foraminiferal distribution in two estuarine intertidal mudflats of the French Atlantic coast: testing the marine influence index. Water 14, 645. https://doi.org/10.3390/w14040645.

Glock, N., 2023. Benthic foraminifera and gromiids from oxygen-depleted environments – survival strategies, biogeochemistry and trophic interactions. Biogeosciences 20, 3423–3447. https://doi.org/10.5194/bg-20-3423-2023.

Goës, A.T., 1894. A Synopsis of the Arctic and Scandinavian Recent Marine Foraminifera Hitherto Discovered. P.A. Norstedt & söner, Stockholm.

Goineau, A., Gooday, A.J., 2019. Diversity and spatial patterns of foraminiferal assemblages in the eastern Clarion-Clipperton zone (abyssal eastern equatorial Pacific). Deep-Sea Res. Part I 149, 103036. https://doi.org/10.1016/j.dsr.2019.04.014.

Goldstein, S.T., Alve, E., 2011. Experimental assembly of foraminiferal communities from coastal propagule banks. Mar. Ecol. Prog. Ser. 437, 1–11. https://doi.org/10.3354/meps09296.

Goldstein, S.T., Barker, W.W., 1988. Test ultrastructure and taphonomy of the monothalamous agglutinated foraminifer *Cribrothalammina,* n. gen., *alba* (Heron-Allen and Earland). J. Foramin. Res. 18, 130–136. https://doi.org/10.2113/gsjfr.18.2.130.

Goldstein, S.T., Barker, W.W., 1990. Gametogenesis in the monothalamous agglutinated foraminifer *Cribrothalammina alba*. J. Protozool. 37, 20–27. https://doi.org/10.1111/j.1550-7408.1990.tb01108.x.

Goldstein, S.T., Habura, A., Richardson, E.A., Bowser, S.S., 2010. *Xiphophaga minuta* and *X. allominuta* nov. gen., nov. spp., new monothalamid foraminifera from coastal Georgia (USA): cryptic species, gametogenesis and an unusual form of chloroplast sequestration. J. Foramin. Res. 40, 3–15. https://doi.org/10.2113/gsjfr.40.1.3.

Gooday, A.J., 2002. Organic-walled allogromiids: aspects of their occurrence, diversity and ecology in marine habitats. J. Foramin. Res. 32, 384–399. https://doi.org/10.2113/0320384.

Gooday, A.J., Fernando, O.J., 1992. A new allogromiid genus (Rhizopoda: Foraminiferida) from the Vellar Estuary, Bay of Bengal. J. Micropalaeontol. 11, 233–239. https://doi.org/10.1144/jm.11.2.233.

Gooday, A.J., Goineau, A., 2019. The contribution of fine sieve fractions (63–150 μm) to foraminiferal abundance and diversity in an area of the eastern Pacific Ocean licensed for polymetallic nodule exploration. Front. Mar. Sci. 6, 114. https://doi.org/10.3389/fmars.2019.00114.

Gooday, A.J., Jorissen, F.J., 2012. Benthic foraminiferal biogeography: controls on global distribution patterns in deep-water settings. Ann. Rev. Mar. Sci. 4, 237–262. https://doi.org/10.1146/annurev-marine-120709-142737.

Gooday, A.J., Wawrzyniak-Wydrowska, B., 2023. Macrofauna-sized foraminifera in epibenthic sledge samples from five areas in the eastern Clarion-Clipperton Zone (equatorial Pacific). Front. Mar. Sci. 9, 1059616. https://doi.org/10.3389/fmars.2022.1059616.

Gooday, A.J., Holzmann, M., Guiard, J., Cornelius, N., Pawlowski, J., 2004. A new monothalamous foraminiferan from 1000 to 6300m water depth in the Weddell Sea: morphological and molecular characterisation. Deep-Sea Res. Part II 51, 1603–1616. https://doi.org/10.1016/j.dsr2.2004.06.025.

Gooday, A.J., Todo, Y., Uematsu, K., Kitazato, H., 2008. New organic-walled Foraminifera (Protista) from the ocean's deepest point, the Challenger Deep (western Pacific Ocean). Zool. J. Linn. Soc. 153, 399–423. https://doi.org/10.1111/j.1096-3642.2008.00393.x.

Gooday, A.J., Anikeeva, O.V., Pawlowski, J., 2011. New genera and species of monothalamous foraminifera from Balaclava and Kazach'ya Bays (Crimean Peninsula, Black Sea). Mar. Biodivers. 41, 481–494. https://doi.org/10.1007/s12526-010-0075-7.

Gooday, A.J., Holzmann, M., Caulle, C., Goineau, A., Kamenskaya, O., Weber, A.A.T., Pawlowski, J., 2017. Giant protists (xenophyophores, Foraminifera) are exceptionally diverse in parts of the abyssal eastern Pacific licensed for polymetallic nodule exploration. Biol. Conserv. 207, 106–116. https://doi.org/10.1016/j.biocon.2017.01.006.

Gooday, A.J., Schoenle, A., Dolan, J.R., Arndt, H., 2020. Protist diversity and function in the dark ocean: challenging the paradigms of deep-sea ecology with special emphasis on foraminiferans and naked protists. Eur. J. Protistol. 75, 125721. https://doi.org/10.1016/j.ejop.2020.125721.

Gooday, A.J., Lejzerowicz, F.J., Goineau, A., Holzmann, M., Kamenskaya, O., Kitazato, H., Lim, S.-C, Pawlowski, J., Radziejewska, T., Stachowska, T., Wawrzyniak-Wydrowska, B., 2021. The biodiversity and distribution of abyssal benthic foraminifera and their possible ecological roles: a synthesis across the Clarion-Clipperton Zone. Front. Mar. Sci. 8, 634726. doi;https://doi.org/10.3389/fmars.2021.634726.

Gooday, A.J., Holzmann, M., Schwarzgruber, E., Cedhagen, T., Pawlowski, J., 2022. Morphological and molecular diversity of monothalamids (Rhizaria, Foraminifera), including two new species and a new genus, from SW Greenland. Eur. J. Protistol. 86, 125932. https://doi.org/10.1016/j.ejop.2022.125932.

Gouy, M., Guindon, S., Gascuel, O., 2010. SeaView version 4: a multiplatform graphical user interface for sequence alignment and phylogenetic tree building. Mol. Biol. Evol. 27, 221–224. https://doi.org/10.1093/molbev/msp259.

Gschwend, F., Majda, A., Majewski, W., Pawlowski, J., 2016. *Psammophaga fuegia* sp. nov., a new monothalamid foraminifera from the Beagle Channel, South America. Acta Protozool. 55, 101–110. https://doi.org/10.4467/16890027AP.16.009.4944.

Guindon, S., Dufayard, J.F., Lefort, V., Anisimova, M., Hordijk, W., Gascuel, O., 2010. New algorithms and methods to estimate maximum-likelihood phylogenies: assessing the performance of PhyML 3.0. Syst. Biol. 59, 307–321. https://doi.org/10.1093/sysbio/syq010.

Habura, A., Rosen, D.R., Bowser, S.S., 2004. Predicted secondary structure of the foraminiferal SSU 3′ major domain reveals a molecular synapomorphy for granuloreticulosean protists. J. Eukaryot. Microbiol. 51, 464–471. https://doi.org/10.1111/j.1550-7408.2004.tb00397.x.

Habura, A., Goldstein, S.T., Broderick, S., Bowser, S.S., 2008. A bush, not a tree: the extraordinary diversity of cold-water basal foraminiferans extends to warm-water environments. Limnol. Oceanogr. 53, 1339–1351. https://doi.org/10.4319/lo.2008.53.4.1339.

Hayward, B.W., Holzmann, M., 2023. Biogeography and species durations of selected Cenozoic shallow and deep-water smaller calcareous benthic foraminifera – a review. J. Foramin. Res. 53, 192–213. https://doi.org/10.2113/gsjfr.53.3.192.

Henderson, Z., 2023. Soft-walled monothalamid foraminifera from the intertidal zones of the Lorn area, north-west Scotland. J. Mar. Biol. Assoc. U.K. 103, e18. https://doi.org/10.1017/S0025315423000061.

Heron-Allen, E., Earland, A., 1932. Foraminifera: Part I. The ice-free area of the Falkland Islands and adjacent seas. Discovery Reports Vol. IV. Cambridge University Press, Cambridge, pp. 291–460.

Himmighofen, O.E., Holzmann, M., Barrenechea-Angeles, I., Pawlowski, J., Gooday, A.J., 2023. An integrative taxonomic survey of benthic foraminiferal species (Protista, Rhizaria) from the eastern Clarion-Clipperton zone. J. Mar. Sci. Eng. 11, 2038. doi; https://doi.org/10.3390/jmse11112038.

Höglund, H., 1947. Foraminifera in the Gullmar Fjord and the Skagerak. Zool. Bidr. Uppsala 26, 1–328.

Holzmann, M., 2024. Isolation, DNA extraction, amplification and gel electrophoresis of single-celled nonmarine foraminifera (Rhizaria). In: Amaresan, N., Chandarana, K.A. (Eds.), Practical Handbook on Soil Protists. Humana Press, New York, NY, pp. 181–188. https://doi.org/10.1007/978-1-0716-3750-0_31.

Holzmann, M., Siemensma, F., 2025. A new freshwater monothalamid (Rhizaria, Foraminifera) from the Pyrenees branching within a marine clade. Eur. J. Protistol. 99, 126156. https://doi.org/10.1016/j.ejop.2025.126156.

Holzmann, M., Gooday, A.J., Siemensma, F., Pawlowski, J., 2021. Review: freshwater and soil foraminifera – a story of long-forgotten relatives. J. Foramin. Res. 51, 318–331. https://doi.org/10.2113/gsjfr.51.4.318.
Holzmann, M., Gooday, A.J., Majewski, W., Pawlowski, J., 2022. Molecular and morphological diversity of monothalamous foraminifera from South Georgia and the Falkland Islands: description of four new species. Eur. J. Protistol. 85, 125909. https://doi.org/10.1016/j.ejop.2022.125909.
Holzmann, M., Nguyen, N.-L., Angeles, I.B., Pawlowski, J., 2024. BFR2: a curated ribosomal reference dataset for benthic foraminifera. Sci. Data 11, 1292. https://doi.org/10.1038/s41597-024-04137-8.
Holzmann, M., Gooday, A.J., Pawlowski, J., 2025a. *Flaviatella* gen. nov., a new genus of monothalamous foraminifera with a wide geographical and bathymetrical distribution. Prog. Oceanogr. 239, 103589. https://doi.org/10.1016/j.pocean.2025.103589.
Holzmann, M., Holm, V.D., Barrenechea Angeles, I., Gooday, A.J., Pawlowski, J., Panieri, G., 2025b. DNA barcoding of monothalamid foraminifera from Vestnesa and Svyatogor ridge, Arctic Ocean, including the description of 3 new species. Polar Biol. 48, 12. https://doi.org/10.1007/s00300-024-03320-2.
ICZN, 1999. International Code of Zoological Nomenclature, 4th ed. International Trust for Zoological Nomenclature, London.
Jorissen, F.J., Fouet, M.P.A., Singer, D., Howa, H., 2022. The marine influence index (MII): a tool to assess estuarine intertidal mudflat environments for the purpose of foraminiferal biomonitoring. Water 14, 676. https://doi.org/10.3390/w14040676.
Kaushik, T., Dixit, V., Murugan, T., 2024. Morphology and molecular phylogeny of two new species of *Psammophaga* (Rhizaria, Foraminifera) from the west coast of India. Eur. J. Protistol. 92, 126035. https://doi.org/10.1016/j.ejop.2023.126035.
Korsun, S., Hald, M., Golikova, E., Yudina, A., Kuznetsov, I., Mikhailov, D., Knyazeva, O., 2014. Intertidal foraminiferal fauna and the distribution of Elphidiidae at Chupa Inlet, western White Sea. Mar. Biol. Res. 10, 153–166. https://doi.org/10.1080/17451000.2013.814786.
Kumar, S., Stecher, G., Tamura, K., 2016. MEGA7: Molecular evolutionary genetics analysis Version 7.0 for bigger datasets. Mol. Biol. Evol. 33, 1870–1874. https://doi.org/10.1093/molbev/msw054.
Larkin, K.E., Gooday, A.J., 2004. Soft-shelled monothalamous foraminifera at an intertidal site on the south coast of England. J. Micropalaeontol. 23, 135–137. https://doi.org/10.1144/jm.23.2.135.
Lee, J.J., Muller, W.A., Stone, R.J., McEnery, M.E., Zucker, W., 1969. Standing crop of foraminifera in sublittoral epiphytic communities of a Long Island salt marsh. Mar. Biol. 4, 44–61. https://doi.org/10.1007/BF00372165.
Lefort, V., Longueville, J.-E., Gascuel, O., 2017. SMS: Smart Model Selection in PhyML. Mol. Biol. Evol. 34, 2422–2424. https://doi.org/10.1093/molbev/msx149.
Lejzerowicz, F., Pawlowski, J., Fraissinet-Tachet, L., Marmeisse, R., 2010. Molecular evidence for widespread occurrence of foraminifera in soils. Environ. Microbiol. 12, 2518–2525. https://doi.org/10.1111/j.1462-2920.2010.02225.x.
Lena, H., 1974. *Dahlgrenia patagoniensis* gen. nov., sp. nov. (Foraminifera, Saccamminidae). Physis, Secc. A (Buenos Aires) 33 (86), 9–16.
Loeblich, A.R., Tappan, H., 1987. Foraminiferal Genera and their Classification. Spinger, New York, NY.
Majewski, W., Pawłowski, J., Zajaczkowski, M., 2005. Monothalamous foraminifera from West Spitsbergen fjords, Svalbard: a brief overview. Pol. Polar Res. 26, 269–285.
Majewski, W., Lecroq, B., Sinniger, F., Pawlowski, J., 2007. Monothalamous foraminifera from Admiralty Bay, King George Island, West Antarctica. Pol. Polar Res. 28, 187–210.
Murray, J.W., 1983. Population dynamics of benthic foraminifera: results from the Exe Estuary, England. J. Foramin. Res. 13, 1–12. https://doi.org/10.2113/gsjfr.13.1.1.
Murray, J.W., 2006. Ecology and Applications of Benthic Foraminifera. Cambridge University Press, Cambridge.
Nyholm, K.G., 1955. Studies on recent Allogromiidae (4), *Phainogullmia aurata* n. gen., n. sp. Zool. Bidr. Uppsala 30, 465–474.
Ohkawara, N., Kitazato, H., Uematsu, K., Gooday, A.J., 2009. A minute new species of *Saccammina* (monothalamous Foraminifera; Protista) from the abyssal Pacific. J. Micropalaeontol. 28, 143–151. https://doi.org/10.1144/jm.28.2.143.
Pavel, A.B., Kreuter, S., Holzmann, M., Enache, A., Motoc, R., Pawlowski, J., 2023. *Psammophaga secriensia* sp. nov., a new monothalamid Foraminifera (Protista, Rhizaria) from the Romanian Black Sea shelf. J. Mar. Sci. Eng. 11, 1546. https://doi.org/10.3390/jmse11081546.
Pawlowski, J., Holzmann, M., 2008. Diversity and geographic distribution of benthic foraminifera: a molecular perspective. Biodivers. Conserv. 17, 317–328. https://doi.org/10.1007/s10531-007-9253-8.
Pawlowski, J., Holzmann, M., 2014. A plea for DNA barcoding of foraminifera. J. Foramin. Res. 44, 62–67. https://doi.org/10.2113/gsjfr.44.1.62.
Pawlowski, J., Majewski, W., 2011. Magnetite-bearing foraminifera from Admiralty Bay, West Antarctica, with description of *Psammophaga magnetica*, sp. nov. J. Foramin. Res. 41, 3–13. https://doi.org/10.2113/gsjfr.41.1.3.
Pawlowski, J., Holzmann, M., Berney, C., Fahrni, J., Cedhagen, T., Bowser, S.S., 2002. Phylogeny of allogromiid foraminifera inferred from SSU rRNA gene sequences. J. Foramin. Res. 32, 334–343. https://doi.org/10.2113/0320334.
Pawlowski, J., Holzmann, M., Berney, C., Fahrni, J., Gooday, A.J., Cedhagen, T., Habura, A., Bowser, S.S., 2003. The evolution of early foraminifera. Proc. Natl. Acad. Sci. U.S.A. 100, 11494–11498. https://doi.org/10.1073/pnas.2035132100.
Pawlowski, J., Bowser, S.S., Gooday, A.J., 2007. A note on the genetic similarity between shallow- and deep-water *Epistominella vitrea* (Foraminifera) in the Antarctic. Deep-Sea Res. Part II 54, 1720–1726. https://doi.org/10.1016/j.dsr2.2007.07.016.
Pawlowski, J., Majewski, W., Longet, D., Guiard, J., Cedhagen, T., Gooday, A.J., Korsun, S., Habura, A.A., Bowser, S.S., 2008. Genetic differentiation between Arctic and Antarctic monothalamous foraminiferans. Polar Biol. 31, 1205–1216. https://doi.org/10.1007/s00300-008-0459-3.
Pawlowski, J., Christen, R., Lecroq, B., Bachar, D., Shahbazkia, H.R., Amaral-Zettler, L., Guillou, L., 2011. Eukaryotic richness in the abyss: insights from pyrotag sequencing. PLoS ONE 6, e18169. https://doi.org/10.1371/journal.pone.0018169.
Pawlowski, J., Holzmann, M., Tyszka, J., 2013. New supraordinal classification of foraminifera: molecules meet morphology. Mar. Micropaleontol. 100, 1–10. https://doi.org/10.1016/j.marmicro.2013.04.002.
Pawlowski, J., Lejzerowicz, F., Esling, P., 2014. Next-generation environmental diversity surveys of foraminifera: preparing the future. Biol. Bull. 227, 93–106. https://doi.org/10.1086/bblv227n2p93.
Pawlowski, J., Gooday, A.J., Holzmann, M., 2025. Massive occurrence of a new soft-walled monothalamous foraminifer, *Bathyallogromia brandtae* n. sp., in the hadal Aleutian trench. Prog. Oceanogr. 235, 103493. https://doi.org/10.1016/j.pocean.2025.103493.
Phleger, F.B., 1960. Ecology and Distribution of Recent Foraminifera. John Hopkins Press, Baltimore.
Ranju, R., Menon, N.R., Nashad, M., Nisha, N.R., 2017. First report of *Ovammina opaca* Dahlgren 1962, a saccamminid benthic foraminiferal species from the sediments of the Arabian Sea. J. Mar. Biol. Mar. Assoc. Ind. 59, 119–122. https://doi.org/10.6024/jmbai.2017.59.2.1964-16.
Rhumbler, L., 1935. Rhizopoden der Kieler Bucht, gesammelt durch A. Remane, I. Teil. Schr. Naturwiss. Ver. Schlesw.-Holst. 21, 143–194.
Sabbatini, A., Pawlowski, J., Gooday, A.J., Piraino, S., Bowser, S.S., Morigi, C., Negri, A., 2004. *Vellaria zucchellii* sp. nov. a new monothalamous foraminifer from Terra Nova Bay, Antarctica. Antarct. Sci. 16, 307–312. https://doi.org/10.1017/s0954102004002081.
Sabbatini, A., Negri, A., Bartolini, A., Morigi, C., Boudouma, O., Dinelli, E., Florindo, F., Galeazzi, R., Holzmann, M., Lurcock, P.C., Massaccesi, L., Pawlowski, J., Rocchi, S., 2016. Selective zircon accumulation in a new benthic foraminifer, *Psammophaga zirconia*, sp. nov. Geobiology 14, 404–416. https://doi.org/10.1111/gbi.12179.
Scheckenbach, F., Hausmann, K., Wylezich, C., Weitere, M., Arndt, H., 2009. Large-scale patterns in biodiversity of microbial eukaryotes from the abyssal sea floor. Proc. Natl. Acad. Sci. U.S.A. 107, 115–120. https://doi.org/10.1073/pnas.0908816106.
Sergeeva, N.G., Anikeeva, O.V., 2024. Soft-Walled Foraminifera and the Gromiids of the Black Sea and the Sea of Azov: Aspects of Taxonomical Diversity and Ecology. Turkish Marine Research Foundation (TUDAV), İstanbul.
Siddall, J.D., 1880. On *Shepheardella*, an undescribed type of marine Rhizopoda with a few observations on *Lieberkiihnia*. J. Cell Sci. (Ser. 2) 20, 130–145. https://doi.org/10.1242/jcs.s2-20.78.130.
Siemensma, F., Holzmann, M., 2023. Novel contributions to the molecular and morphological diversity of freshwater monothalamid foraminifera: description of six new species. Eur. J. Protistol. 90, 126014. https://doi.org/10.1016/j.ejop.2023.126014.
Siemensma, F., Apothéloz-Perret-Gentil, L., Holzmann, M., Clauss, S., Völcker, E., Pawlowski, J., 2017. Taxonomic revision of freshwater foraminifera with the description of two new agglutinated species and genera. Eur. J. Protistol. 60, 28–44. https://doi.org/10.1016/j.ejop.2017.05.006.
Siemensma, F., Holzmann, M., Apothéloz-Perret-Gentil, L., Clauß, S., Voelcker, E., Bettighofer, W., Khanipour Roshan, S., Walden, S., 2021. Broad sampling of monothalamids (Rhizaria, Foraminifera) gives further insight into diversity of non-marine foraminifera. Eur. J. Protistol. 77, 125744. https://doi.org/10.1016/j.ejop.2020.125744.
Singer, D., Fouet, M.P.A., Schweizer, M., Mouret, A., Quinchard, S., Jorissen, F.J., 2023. Unlocking foraminiferal genetic diversity on estuarine mudflats with eDNA metabarcoding. Sci. Total Environ. 902, 165983. https://doi.org/10.1016/j.scitotenv.2023.165983.
Sinniger, F., Lecroq, B., Majewski, W., Pawlowski, J., 2008. *Bowseria arctowskii* gen. et sp. nov., new monothalamous foraminiferan from the Southern Ocean. Pol. Polar Res. 29, 5–15.
Stachowska-Kamińska, Z., Gooday, A.J., Radziejewska, T., Arbizu, P.M., 2022. Macrofaunal foraminifera from a former benthic impact experiment site (IOM contract area) in the abyssal eastern Clarion-Clipperton Zone. Deep-Sea Res. Part I 188, 103848. https://doi.org/10.1016/j.dsr.2022.103848.
Voltski, I., Pawlowski, J., 2015. *Flexammina islandica* gen. nov. sp. nov. and some new phylotypes of monothalamous foraminifera from the coast of Iceland. Zootaxa 3964, 245–259. https://doi.org/10.11646/zootaxa.3964.2.5.
Whitfield, A.K., Elliott, M., 2011. Ecosystem and biotic classifications of estuaries and coasts. In: Wolanski, E., McLusky, D.S. (Eds.), Treatise on Estuarine and Coastal Science. Academic Press, Waltham, pp. 99–124.
Wilding, T., 2002. Taxonomy and ecology of *Toxisarcon alba* sp. nov. from Loch Linnhe, west coast of Scotland, UK. J. Foramin. Res. 32, 358–363. https://doi.org/10.2113/0320358.
Yang, H., Peng, X., Gooday, A.J., Jones, B., Li, J., Liu, S., Huang, W., Sun, Z., Chen, S., Dasgupta, S., Xu, H., Liu, S., Xu, W., Ta, K., 2022. Magnetic foraminifera thrive in the Mariana Trench. Geochem. Perspect. Lett. 21, 23–27. https://doi.org/10.7185/geochemlet.2212.